Polymer Fiber based Sensors

Miguel Fernandes Soares Ferreira
Integrated Master's in Engineering Physics
Physics and Astronomy Department
2016

Supervisor
Orlando José Reis Frazão, Invited Assistant Professor, Faculty of Sciences of the University of Porto

Co-Supervisor
Manuel Joaquim Bastos Marques, Assistant Professor, Faculty of Sciences of the University of Porto

Todas as correções determinadas pelo júri, e só essas, foram efetuadas.
O Presidente do Júri,

Porto, _____/_____/_____

Acknowledgements

To my supervisor, Dr. Orlando Frazão, who introduced me to investigation and challenged me in my work, always had a plan B and solved problems in somewhat mysterious ways and to my co-supervisor, Manuel Marques, who helped me with bureaucracy and technical problems and always had a funny story to tell.

To my friends and colleagues André Gomes, João Maia, Miguel Amaral and Vítor Amorim, who stood by my side and helped me when I needed the most. To André Gomes, António Rodrigues, Catarina Monteiro, Regina Magalhães and Tiago Martins, that provided a good environment to work, for their teamwork and funny moments. To António Rodrigues, for his help every single time I bother him with software problems. To Catarina Monteiro, who was always by my side, supporting me, cheering me up and did her best to help me.

To my colleagues both in Porto and Wrocław, Dominik Kowal and Dr. Gabriela Statkiewicz-Barabach, for all they taught me about this subject and, along with Dr. Szymon Barabach, Dr. Alicja Anuszkiewicz and Dr. Wacław Urbanczyk, for their hospitality and help when I was in Wrocław.

To INESC-TEC, more specifically CAP, for the work conditions and the professional environment and the opportunity to develop my dissertation and to D. Luísa Mendonça, for all the bureaucracy she helped me with, and her motivational conversations.

To my best friend, André Cosme, who always made his best to cheer me up when things went wrong and made me look at the bright side of every situation.

To my parents, without them this would be impossible, for their support and patience when I was grumpy due to stress from this work and to my not so little brother, for the times he was patient when I couldn't play with him.

This work was supported by the grant for bilateral scientific cooperation between Poland and Portugal and in part by Fundação para a Ciência e Tecnologia (Portuguese Foundation for Science and Technology), in part by the European Regional Development Fund (ERDF) through the COMPETE Programme (Operational Programme for Competitiveness) within Project FCOMP-01-0124-FEDER-037281 and supported by Fundos FEDER (FEDER Funds) through the Programa Operacional Competitividade e Internacionalização – COMPETE 2020 within project «POCI-01-0145-FEDER-006961», by Fundos Nacionais (Portuguese Nacional Funds) through FCT – Fundação para a Ciência e a Tecnologia through the project UID/EEA/50014/2013

Resumo

Os sensores em fibra ótica trouxeram várias vantagens na área de sensorização. Geralmente compostas por sílica, as fibras óticas são usadas para a fabricação de dispositivos de sensorização baseados em redes de difração, interferometria ou revestimentos de forma a monitorizar parâmetros externos.

As fibras óticas podem também ser compostas por polímero. As fibras óticas poliméricas demonstram diferentes características e vantagens em relação às fibras de sílica comuns, o que as torna interessantes para a fabricação de sensores. O fabrico e a exploração do uso de sensores baseados em redes de Bragg (FBGs) e redes de período longo (LPGs) em fibras poliméricas são foco do trabalho desta dissertação.

A fabricação de FBGs em fibra polimérica foi estudada usando a técnica de máscara de fase. Os resultados mostram FBGs capazes de serem usados para fins de sensorização. Sensores baseados em FBGs foram testados e apresentam sensibilidade a deformação, temperatura e pressão.

Uma cavidade Fabry-Perot foi formada usando um FBG e a face da ponta da fibra. O interferómetro provou ser sensível a alterações de índice de refração.

A fabricação de LPGs em fibras óticas poliméricas microstruturadas foi estudada recorrendo a duas técnicas, ponto-a-ponto e mecânica. Usando a técnica de ponto-a-ponto, é possível ter controlo sobre os parâmetros da rede e permite a visualização da qualidade da rede após irradiar cada ponto. Usando meio mecânicos, é possível obter LPGs temporários ou permanentes. Redes temporárias podem ser usadas para obter uma pré-visualização do resultado dos parâmetros escolhidos sem arriscar um processo irreversível. Um interferómetro de Mach-Zehnder foi desenvolvido em fibra polimérica inscrevendo duas redes de período longo em série usando a técnica mecânica permanente. O dispositivo resultante provou ser sensível à deformação.

Palavras-chave: Fibra óptica polimérica, sensores de fibra óptica, rede de Bragg em fibra, interferómetro Fabry-Perot, rede de período longo, interferómetro Mach-Zehnder.

Abstract

Optical fiber sensors brought many advantages to the sensing area. Optical fibers are usually composed of silica and are used to create sensing devices through the fabrication of gratings, interferometers or the deposition of coatings in order to monitor external parameters.

Optical fibers can also be composed of polymer. Polymer optical fibers present different characteristics and advantages over standard silica fiber, which makes them interesting for sensor fabrication. The work of this dissertation is to develop and explore the use of polymer fiber based sensors, through the fabrication of fiber Bragg gratings (FBGs) and long period gratings (LPGs).

The fabrication of FBGs in polymer fibers using a phase-mask technique was studied. The results showed FBGs capable of being used for sensing purposes. FBG based sensors were tested and presented sensitivity to strain, temperature and pressure.

A Fabry-Perot cavity was formed between FBG and the end face of the fiber. The interferometer proved to be sensitive to refractive index variation.

LPG fabrication in microstructured polymer optical fiber was studied using two techniques, point-by-point and mechanical. The point-by-point technique gives control over the parameters of the grating and allows monitoring of the quality of the grating after each irradiated point. Through mechanical means, temporary or permanent LPGs can be fabricated. Temporary gratings can be used to have a preview of the result of the chosen parameters without risking an irreversible process. A Mach-Zehnder interferometer was developed in the polymer fiber where two LPGs were inscribed in a row using the permanent mechanical technique. The developed device proved to be strain sensitive.

Keywords: Polymer optical fiber, optical fiber sensors, fiber Bragg grating, Fabry-Perot interferometer, long period grating, Mach-Zehnder interferometer.

Table of Contents

List of Figures

List of Abbreviations

FBG – fiber Bragg grating
FFT – fast Fourier transform
FP – Fabry-Perot
FWHM – Full Width Half Maximum
Hi-Bi – highly birrefringent
LPG – long period grating
OSA – Optical Spectrum Analyzer
PMMA - poly(methyl methacrylate)
POF – Polymer Optical fiber
SC - Supercontinuum
UV – ultraviolet

Chapter 1
Introduction

1.1 Motivation

New sensors developments are supported by the search of more accurate measurements or sensors that can withstand special conditions. Optical fibers present characteristics like small size and immunity to electromagnetic interference, which makes them suitable for sensing applications. Optical fiber sensors operation principle is based on the analysis of variations in the wavelength or optical power of the spectrum caused by a specific parameter change in the fiber.

Optical fibers appeared around the 60s and lead to the first studies on optical fiber sensing [1]. Polymer optical fibers (POFs) present advantages over the commonly used silica fibers. These fibers present smaller Young's Modulus and higher resistance to damage which expand the range of application of optical fiber based sensors [2]. However, the high propagation losses made these fibers unnoticed. Recently, the interest to study POFs as fiber sensors has increased [3–5].

Devices like fiber Bragg gratings (FBGs) and long period gratings (LPGs) inscribed in POFs appeal for the fabrication of POF based sensors. FBG and LPG based sensors have been reported in silica fibers [6–8]. Their combination with POF allows the fabrication of sensors that can take advantage of the characteristics of the polymer fibers.

FBGs and LPGs consist in periodic perturbations inscribed in the fiber, where the FBGs have sub-micron periodicity and while LPGs present periodicities of hundreds of microns. The structure of the FBG reflects a given wavelength and the LPG couples a certain wavelength to the cladding depending on the size of the period and the refractive index of the fiber. This is explored for sensing as parameters can be measured as they alter the period and the effective refractive index. Both gratings are easily and quickly fabricated and easily implemented as sensors.

The study and development of POF sensors is the main theme of this dissertation with a larger focus on FBG and LPG based sensors.

1.2 Aim and Objectives

This dissertation aims to develop optical fiber sensors using polymer optical fibers to apply in the sensing of physical parameters such as strain, temperature, pressure and refractive index.

The objectives established were:

- The development and characterization of FBG based sensors imprinted in polymer fibers;
- The development and characterization of LPG based sensors imprinted in polymer fibers;
- The study of the use of microstructured polymer optical fibers (MPOFs) for sensing applications.

1.3 Structure of the dissertation

This dissertation is divided into six chapters, one of which is the motivation and, at the end, the conclusion and future work. Four chapters present experimental work throughout this dissertation.

Chapter 1 comprises the motivation of this dissertation, the objectives and, finally, the list of publications resulting from this work.

Chapter 2 contains the state-of-art of Polymer Optical Fiber based Sensors. It presents the composition and characteristics of POF and their mark in the history of sensors. An overview through FBGs, LPGs and MPOFs is presented as they are a part of the focus of this dissertation.

In Chapter 3, the work around FBGs imprinted in polymer optical fibers is shown. Fabrication, development and characterization of sensors are the main results obtained. Sensors for strain, temperature and pressure were studied.

In Chapter 4, a Fabry-Perot (FP) interferometer was developed fabricating a cavity between an FBG and the end face of the fiber and characterized for refractive index measurements.

Chapter 5 focuses on LPGs in MPOF. It presents two types of techniques for LPG fabrication, the development of a Mach-Zehnder interferometer and characterization in strain sensing.

In Chapter 6, concluding remarks of this work are presented, followed by future work possibilities.

1.4 Outputs

Ferreira, M. F. S., Statkiewicz-Barabach, G., Kowal, D., Frazão, O., Refractive Index Sensing Using FBG based Fabry-Perot in Polymer Fiber. XIII Symposium on Enabling Optical Networks and Sensors (SEONS 2016), Universidade da Beira Interior, Covilhã, Portugal, 8 July 2016 (Oral Presentation).

Ferreira, M. F. S., Statkiewicz-Barabach, G., Kowal, D., Frazão, O., Mergo, P., Urbanczyk, W., Refractive Index Sensor using a Fabry-Perot cavity in Polymer Fiber. (Submitted publication in OFS).

Ferreira, M. F. S., Statkiewicz-Barabach, G., Kowal, D., Frazão, O., Mergo, P., Urbanczyk, W., Fabry-Perot cavity based on Polymer FBG as Refractive Index Sensor. (Pending publication in Optics Communications).

Chapter 2
State-of-art

Optical fibers are a useful mean of sending information through long distances and a tool to fabricate different kinds of sensors. Conventional optical fibers are made of doped silica and present small dimensions, low weight and immunity to electromagnetic interference. These fibers open the possibility to have sensors where the conditions are not appropriated to traditional electrical sensors, whether for the dangers or for the interference in the environment.

An uncommon type of optical fibers are polymer fibers, usually composed of poly(methyl methacrylate) (PMMA) but also polystyrene and polycarbonates [9]. These fibers often have larger dimensions and have higher transmission losses than silica fibers, but are sturdier, more biocompatible and present a smaller Young's Modulus. Thus, in this dissertation, the goal is to fabricate and characterize polymer fiber based sensors.

FBGs and LPGs can be used as sensors by tracking their wavelength's shifts with variations of external physical parameters like strain, temperature, pressure, refractive index among others. Besides solid core polymer fibers, MPOFs are also produced. These fibers possess advantages that can be explored.

In this chapter the aim is to explore the use of POF for fiber optics sensors, the past of POF based sensors and the working principle of LPGs and FBGs followed by examples of sensors found in literature. A presentation of MPOFs, its advantages and uses are demonstrated.

2.1 Polymer Optical Fiber

Polymer Optical Fibers have been around for the same time as standard silica optical fibers, but silica fibers are the most commonly used [9]. One of the main disadvantages of POF is the high attenuation, the transmission in these fibers is around 520-780 nm. The attenuation ranges from 0.125 dB/m (125 dB/km), in PMMA, to 1 dB/m (1000 dB/km), in polystyrene and polycarbonates. This, compared to silica fibers with less than 0.0002 dB/m (0.2 dB/km) of losses, makes them less competitive [10]. PMMA works better at the visible range where the material absorption is smaller (Fig. 2.1).

The dependence with wavelength of refractive index of PMMA has been studied several times over the years as seen in Figure 2.2 and presents a non-linear behavior [11]. Polymer fibers have larger diameter of the cladding and core than silica fibers, this makes it easier to couple the light into the core. In Figure 2.3 is shown an alignment between a SMF-28, with a diameter of 125 μm and a POF with around the double of the diameter. These fibers are also more elastic than silica fibers, with a Young's Modulus rounding the 3 GPa [2, 12, 13]. They can withstand more force without getting damaged and can be stretched longer as well.

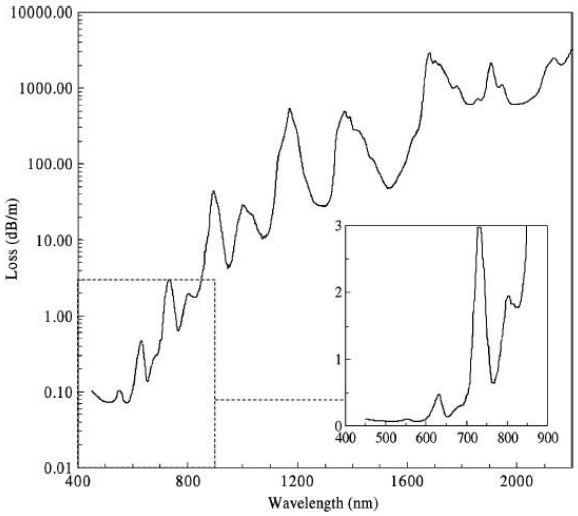

Fig. 2.1 - PMMA material absorption [6].

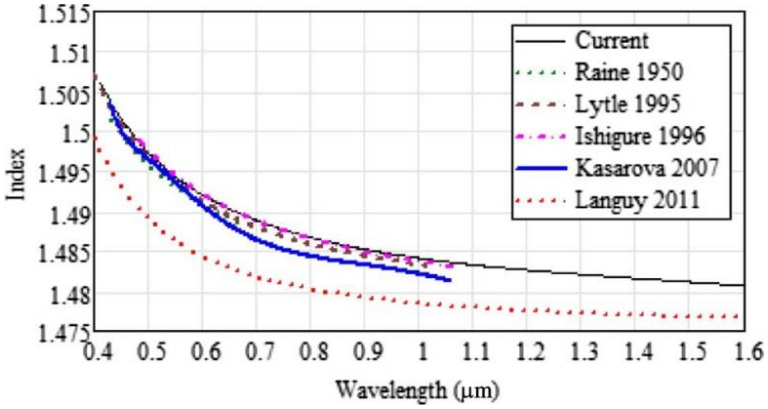

Fig. 2.2 – Refractive index of PMMA [11].

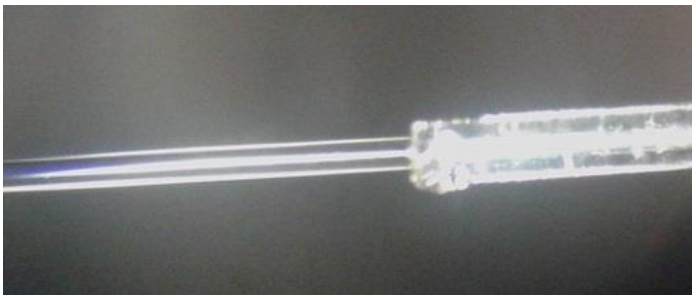

Fig. 2.3 – Comparison between a SMF-28, on the left, and a polymer fiber, on the right.

2.2 Fiber Bragg Grating

A Fiber Grating is a periodic perturbation introduced by inducing a variation in the refractive index of the core. Also known as Short-Period Fiber Gratings, Fiber Bragg Gratings have sub-micron periods and are usually used as single wavelength mirrors [14] . In Figure 2.4, an example of the working principle of the FBG is presented.

As the name suggests, FGBs follow Bragg Law. In the classic experiment, when an electromagnetic wave has a wavelength of the order of the atomic plane spacing of a crystalline material Bragg diffraction occurs. This only occurs when the interference of the wave diffracted in each parallel atomic plane interferes constructively. According to Bragg law this happens when:

$$m\lambda = 2d \sin\theta, \qquad (2.1)$$

where d is the atomic plane spacing, m is an integer and θ is the incident angle.

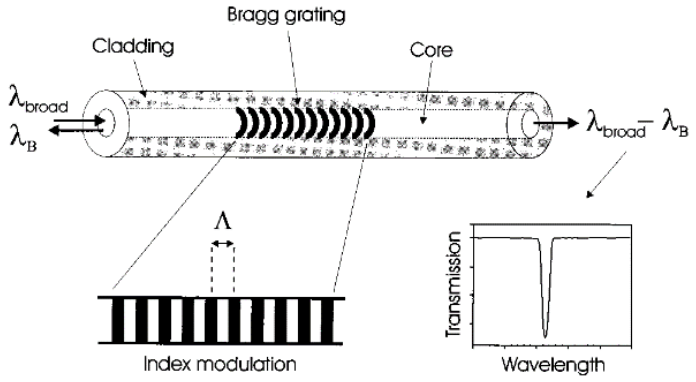

Fig. 2.4- Illustration of a uniform Bragg grating with constant index modulation amplitude and period [14].

In the case of FBGs, a Fresnel reflection occurs in each perturbation where the wave is perpendicular to its plane, $\theta = 90°$. For $m = 1$, from Eq. (2.1), $\lambda = 2d$ is obtained, but since the spacing between the perturbation planes is equal to the grating's period and taking the fiber medium, $d = n_{eff}\Lambda$, so, for FBGs, the following condition is reached:

$$\lambda_B = 2n_{eff}\Lambda, \tag{2.2}$$

where λ_B is the Bragg wavelength, the wavelength that is reflected by the FBG [15].

2.2.1 Conventional FBG sensors

Since a FBG reflects a certain wavelength, dependent of the parameters of the fiber and of the FBG, it is possible to monitor wavelength shifts either by analyzing the reflected or the transmitted spectrum. According to Eq. (2.2) λ_B will change if there is a variation in the effective refractive index or in the periodicity.

The refractive index of the fiber, n, and the periodicity of the FBG, Λ, are both dependent of strain and temperature. For a fiber of length l, from Eq. (2.2) is possible to obtain the shift of the Bragg wavelength [14]:

$$\Delta\lambda_B = 2\left(\Lambda\frac{\partial n}{\partial l} + n\frac{\partial \Lambda}{\partial l}\right)\Delta l + 2\left(\Lambda\frac{\partial n}{\partial T} + n\frac{\partial \Lambda}{\partial T}\right)\Delta T. \tag{2.3}$$

On the right side, the first term of Eq. (2.3) is the dependence of the Bragg wavelength on the applied strain and the second term on the temperature change. An experiment obtained, with $\lambda_B \approx 1551\,\mathrm{nm}$, a strain sensitivity of $9\times10^{-4}\ \mathrm{nm/\mu\varepsilon}$ [16]. Normalized temperature sensitivity at constant strain can be found to be $6.67\times10^{-6}\ ^{\circ}\mathrm{C}^{-1}$ [17]. FBG based sensors include curvature sensors, with a sensitivity of $48.9\ \mathrm{pm/m^{-1}}$ for FBGs with $\lambda \approx 1564\,\mathrm{nm}$ [18], and pressure sensors, with a pressure sensitivity of $0.020\ \mathrm{nm/MPa}$ for a highly birefringent (Hi-Bi) fiber with central wavelength ($\lambda_{Fast} = 1556.82\,\mathrm{nm}$ and $\lambda_{Slow} = 1557.59\,\mathrm{nm}$) [19].

2.2.2 FBGs in Polymer Fibers

The interest in exploring POFs to create FBGs has been growing in the past years. The aim to explore the advantages of POF over Standard Optical Fiber has led to exploring the fabrication of FBG based sensors on polymer fiber by analyzing the spectrum of the FBG. Figure 2.5 shows the reflected spectrum with a Bragg wavelength of $1561.50\,\mathrm{nm}$ and a Full Width Half Maximum (FWHM) bandwidth of $8.78\,\mathrm{nm}$.

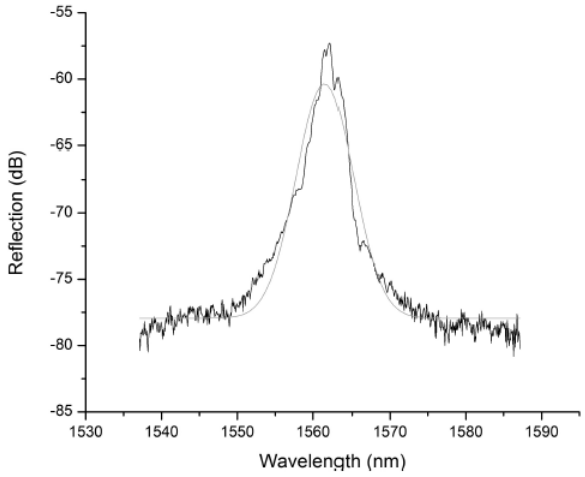

Fig. 2.5- Reflectivity of a polymer FBG and a Gaussian fit [20].

A Bragg grating imprinted on an eccentric-cored polymer optical fiber was reported [3]. The sensor achieved a strain sensitivity of $11.3 \pm 0.1\ \mathrm{nm}/\%$ for $\lambda_B = 1562.5\ \mathrm{nm}$. Tests comparing annealed with non-annealed polymer fibers, composed by PMMA and a core doped with polystyrene, showed similar results between both with a strain sensitivity of $1.37\ \mathrm{pm}/\mu\varepsilon$ and $1.3\ \mathrm{pm}/\mu\varepsilon$, respectively [21].

Thermal characteristics of Bragg gratings structures fabricated in polymer fibers were tested. Temperature sensitivities of $-77\ \mathrm{pm}/℃$ were obtained [22]. Other reports on an eccentric-cored polymer optical fiber showed thermal responses of $-50.1\ \mathrm{pm}/℃$ for $\lambda_B = 1562.5\ \mathrm{nm}$ at $T = 18℃$ [3] (Fig. 2.6). The negative sensitivity is due to a larger dependence of the refractive index to the temperature, which makes the refractive index drop while the temperature increases. Thermal sensitivity between annealed and non-annealed PMMA, with polystyrene doped core, optical fiber Bragg grating was also studied and registered as $-98\ \mathrm{pm}/℃$ for the annealed fibers and $-109\ \mathrm{pm}/℃$ for the non-annealed fibers [21].

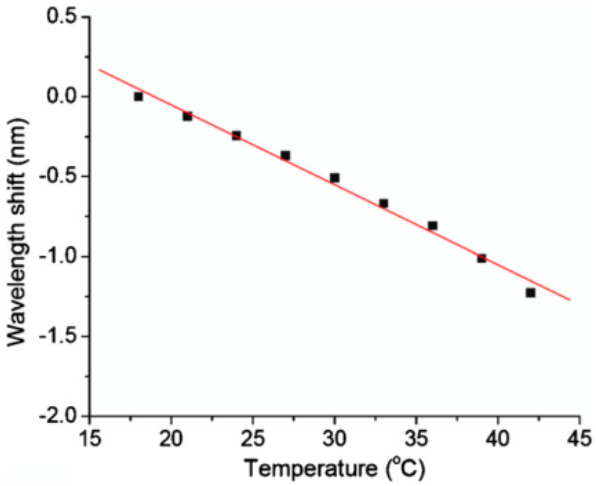

Fig. 2.6- Bragg wavelength shift against temperature [3].

PMMA fibers with eccentric core obtained a high curvature sensitivity of $-63.3\ \mathrm{pm/m^{-1}}$ in a curvature range of $\pm 22.7\ \mathrm{m^{-1}}$ and detected an orientation dependence for $\lambda_B = 1562.5\ \mathrm{nm}$ [3]. Hydrostatic pressure sensitivity of FBGs in POF was also studied and compared with their silica counterparts (Fig 2.7). Up to $10\ \mathrm{MPa}$, the POF sensor showed for a pressure sensitivity of $130 \times 10^{-3}\ \mathrm{pm/MPa}$, larger than the $-3.88\ \mathrm{pm/MPa}$ in silica [20].

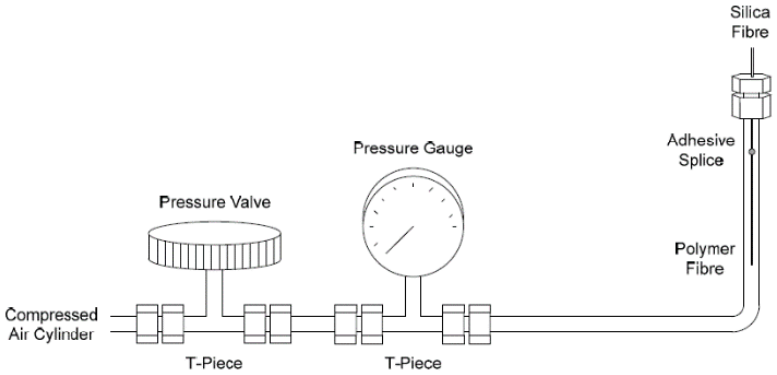

Fig. 2.7- Experimental setup to test the hydrostatic pressure sensitivity of polymer optical fiber Bragg gratings [20].

2.3 Long Period Grating

Long Period Gratings are another kind of grating structure. LPGs are fiber gratings with periods that can range from tens of micrometers to a few millimeters (Fig. 2.8). This periodic perturbation allows core modes to be coupled to the cladding (Fig. 2.9), the high attenuation of the cladding causes a transmission drop at certain wavelengths. The wavelengths with low transmission signal are the ones coupled to the cladding, its phase-matching condition is given by:

$$\lambda(m) = \left(n_{eff} - n_{cl}(m)\right)\Lambda, \qquad (2.4)$$

where $\mathrm{n_{eff}}$ is the effective refractive index of the core mode at the wavelength λ, $\mathrm{n_{cl}(m)}$ is the index refractive index of the cladding m mode and Λ is the LPG periodicity [23]. There are several methods to alter the core's refractive index like ultraviolet (UV), CO_2 laser or infrared femtosecond pulses irradiation, dopant diffusion and electrical discharges [24].

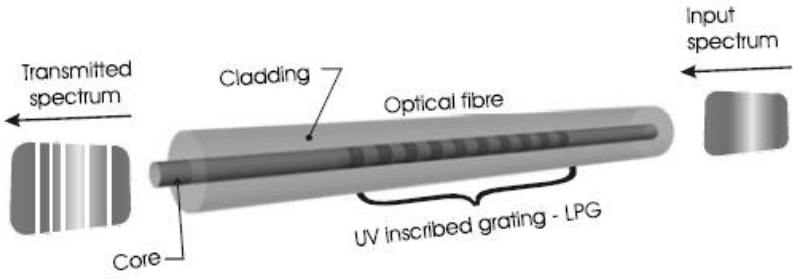

Fig. 2.8- LPG's schematics [24].

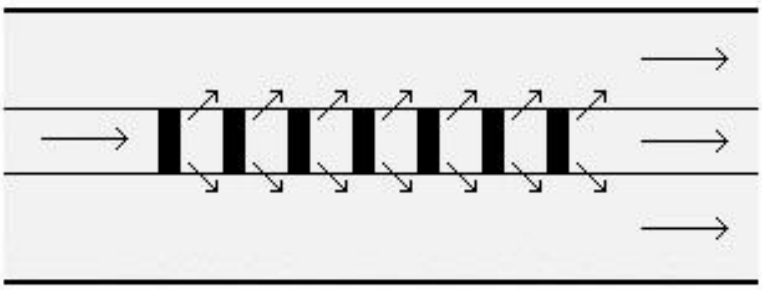

Fig. 2.9 – Schematic of the working principles of an LPG.

2.3.1 Conventional LPG Sensors

LPGs can be used as sensors, since the cut-off wavelengths follow Eq. (2.4). Variations in n_{eff}, n_{cl} or Λ will cause a shift in the spectrum and can be due to strain, temperature or other parameters. This shift is dependent of the m mode of each cladding mode. For a fiber with length L being stretched, strain sensitivity in an LPG can be easily calculated by deriving Eq. (2.4) in function of strain, $\varepsilon = \frac{\Delta L}{L}$:

$$\frac{d\lambda}{d\varepsilon} = \frac{d\lambda}{d(\delta n_{eff})}\left(\frac{dn_{eff}}{d\varepsilon} - \frac{dn_{cl}(m)}{d\varepsilon}\right) + \frac{d\Lambda}{d\varepsilon}\frac{d\lambda}{d\Lambda}, \quad (2.5)$$

where $\delta n_{eff} = n_{eff} - n_{cl}$. Knowing that $\frac{\Delta L}{L} = \frac{\Delta\Lambda}{\Lambda}$, Eq. (2.5) can turn into:

$$\frac{d\lambda}{d\varepsilon} = \frac{d\lambda}{d(\delta n_{eff})}\left(\frac{dn_{eff}}{d\varepsilon} - \frac{dn_{cl}(m)}{d\varepsilon}\right) + \Lambda\frac{d\lambda}{d\Lambda}. \quad (2.6)$$

Strain causes changes in the refractive index of the core and cladding and makes the periodicity increase as the fiber is stretched [25]. These changes give rise to a wavelength shift in which the phase-matching condition occurs. An example of a sensor in the literature [25] shows a maximum strain sensitivity of $-21.44\ \mathrm{nm}/\%$ by tracking the shift of the band at 1141.5 nm . In the right side of Eq. (2.6), the first term shows the grating's refractive index sensitive to axial strain and the second term the

grating's periodicity sensitivity. As for the previous case, the temperature sensitivity can be obtained by deriving Eq. (2.4):

$$\frac{d\lambda}{dT} = \frac{d\lambda}{d(\delta n_{eff})}\left(\frac{dn_{eff}}{dT} - \frac{dn_{cl}(m)}{dT}\right) + \frac{\Lambda}{L}\frac{d\lambda}{d\Lambda}\frac{dL}{dT}. \quad (2.7)$$

As temperature changes the volume of the fiber changes, modifying the periodicity, the effective refractive index and the refractive index of the core [8]. These changes depend on the composition of the fiber, different compositions cause the fiber to react different to the temperature showing different sensitivities. A temperature sensitivity of 405.09 and $410.66\ \mathrm{pm/℃}$ were attained for a half coated, with poly(allylamine hydrochloride) and poly(acrylic acid, sodium salt), LPG [26].

Besides strain and temperature sensors, LPGs can be used for pressure, refractive index and curvature measurements [8, 24]. The fiber when subjected to pressure suffers birefringence. This makes the attenuation band split in two due to the existence of two different phase-matching conditions. A pressure sensitivity of $0.078\ \mathrm{nm/bar}$ can be found in literature [27].

Humidity absorbed by the fiber will make its refractive index change so it is possible to have an LPG based humidity sensor. A humidity sensitivity of $81.61\ \mathrm{pm/(\%RHunit)}$[1] was obtained for an LPG coated with poly(allylamine hydrochloride) and poly(acrylic acid, sodium salt) [24].

Writing two LPGs in a row, some light will couple to the cladding and, then, couple back to the core interfering with the light that is travelling in the core creating a Mach-Zehnder interferometer [28, 29]. The light in the core will travel a different optical path than the light in the cladding and end up interfering with different phases. Sensors based on this principle have been studied in literature [30, 31].

2.3.2 Polymer LPGs

The interest in exploring POFs to create LPGs has been growing in the past years. The advantage of resistance to damage over the Standard Optical Fiber allows for strain sensors to endure larger strains without breaking or deforming [32]. The transmission spectrum of a polymer LPG is presented in Figure 2.10 presents a strength of -13.5 dB centered at 578 nm with a FWHM bandwidth inferior to 4 nm.

[1] RHunit stands for Relative Humidity unit.

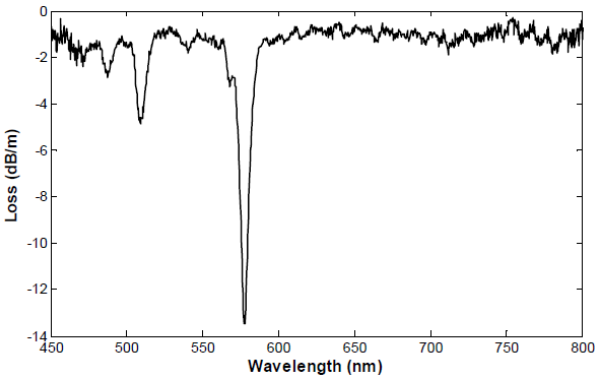

Fig. 2.10- Transmission of a polymer LPG [33].

LPGs started to get more attention since the appeared MPOF and overcame the difficulties of fabricating single-mode fibers [34].

LPGs as strain sensors have been studied. For a mechanically imprinted LPG, a strain sensitivity of $-11\ \mathrm{nm}/\%$ was attained [33] (Fig. 2.11). The negative sensitivity is due to the refractive index change of the cladding being greater than the refractive index in the core when the strain is applied. Other strain tests were done by monitoring the loss feature at 596 nm, achieving a sensitivity of $-5.4\ \mathrm{nm}/\%$ [35].

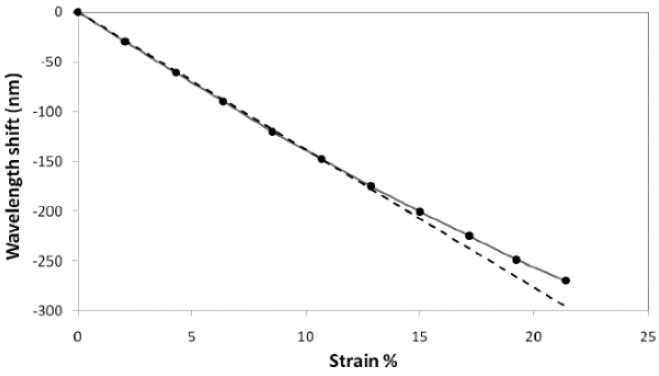

Fig. 2.11- Response of grating wavelength to applied strain. A linear response is observed at low strains, and a deviation from this linearity is observed at higher strains [33].

LPGs written point by point in PMMA doped with azobenzene were also fabricated to test better LPG writing conditions and a strain sensitivity of $-1.57\ \mathrm{nm}/\mathrm{m}\varepsilon$ was achieved [36].

Some tests were done to improve the speed and efficiency of writing LPGs point-by-point by doping the fiber with trans-4-stilbenemethanol. Those LPGs attained a temperature sensitivity of $0.0307\ \mathrm{nm}/℃$ while increasing the temperature and $0.0418\ \mathrm{nm}/℃$ when decreasing the temperature, by tracking the shift from the loss at around 827.8 nm [37].

Tests with reversible LPGs in POF led to the discovery of high transverse strain sensitivity sensors. By applying loads over a grooved plate a pressure sensitivity of

$1.7\ \mathrm{nm/kg}$ was achieved while the fiber remained undamaged up until 12 kg of applied weight [38].

Some single mode POF fibers with imprinted LPGs have been studied for humidity sensing. In a climate chamber at a constant temperature, the POFs were subjected to different percentages of humidity level and a mean humidity sensitivity of $(7.8 \pm 1.6) \times 10^{-4}/(10\ \%)$ was obtained [39].

2.4 Microstructured Polymer Optical Fiber

Photonic Cristal Fibers (PCF) that distinguish themselves from the Standard Optical Fiber for the single material composition and the presence of air holes surrounding the solid core. This avoids problems with doping and allows the possibility of using low-loss materials. An interesting aspect of this fibers is their “endlessly singlemode” properties [40].

The adaptation of MOF into polymer fibers was of great interest. With the first MPOF reported in 2001 [41], several disadvantages of the conventional POF were overcome: the use of only one polymer removes problems with doping and has the potential to reduce absorption losses in the fiber material. Also, although the first MPOF had several small deformations (Fig. 2.12), MPOFs show several advantages over conventional MOFs, like larger drawing temperature ranges without affecting the final structure of the fiber and better control of the shape of the holes.

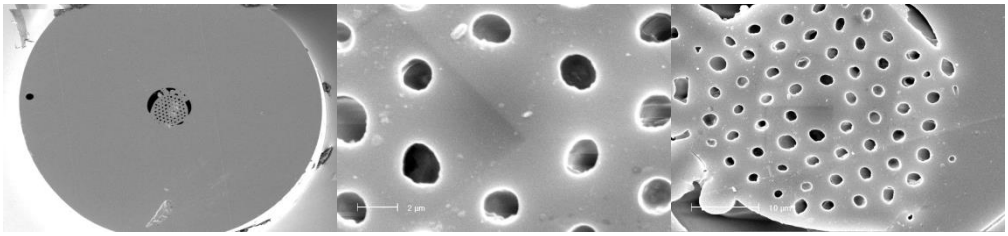

Fig. 2.12- Electron micrographs of the microstructured polymer optical fiber (MPOF) [41].

MPOFs have been fabricated for strain [42, 43], temperature [43, 44] and hydrostatic pressure measurements [43] and have proven capable of being used as biosensors of antibodies [5]. It is possible to detect trapped antibodies in the holes regions through the analysis of fluorescence from the laser excited Cy3-labeled antibodies [5].

A birefringent dual-core MPOF was tested as a sensor. Used as a polarimetric sensor it achieved a strain sensitivity of $3.1\ \mathrm{rad/(m\varepsilon \times m)}$ and an hydrostatic pressure sensitivity of $72\,\mathrm{rad/(MPa \times m)}$. As an intermodal phase sensor, strain sensitivity of $0.9\ \mathrm{rad/(m\varepsilon \times m)}$ and an hydrostatic pressure sensitivity of $13.5\,\mathrm{rad/(MPa \times m)}$ were

achieved. For an annealed fiber an hysteretic temperature sensitivity between $-0.6\ \mathrm{rad/(K \times m)}$ and $0.7\ \mathrm{rad/(K \times m)}$ was attained [43] (Fig. 2.13). With a different hole configuration, a temperature sensitivity of $-2.0\ \mathrm{rad\ m^{-1}K^{-1}}$ for heating and $-1.7\ \mathrm{rad\ m^{-1}K^{-1}}$ for cooling was obtained [44].

A MPOF with an hollow core was first created in 2005 [42]. This fiber, with a length of $30\ \mathrm{cm}$ and a diameter of $330\ \mu\mathrm{m}$, presented in Figure 2.14, was tested for strain sensitivity and the results on Figure 2.15 were obtained.

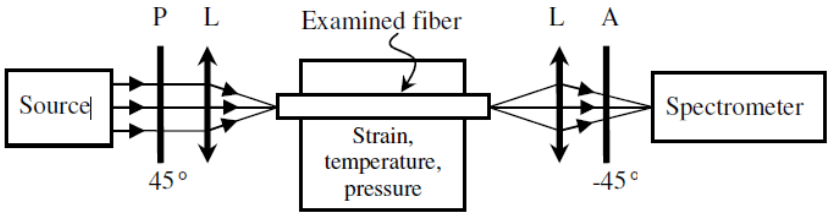

Fig. 2.13- Setup for measurements of birefringence and polarimetric sensitivity to different measurands in each core individually, P-polarizer, A-analyzer, L-microscope objective [43].

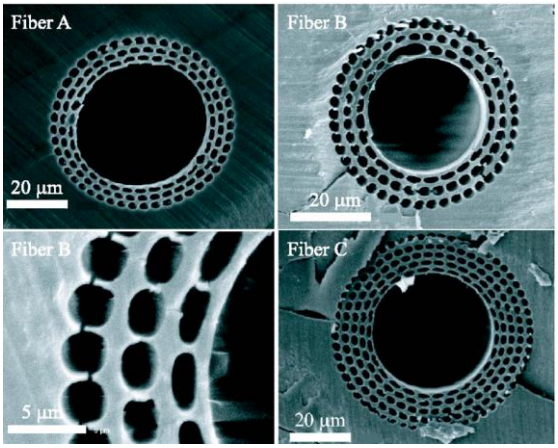

Fig. 2.14- Scanning electron micrographs of the hollow-core MPOFs. Features such as the cracks and the apparent changing thickness of the core boundary are artifacts arising from the cleaving [42].

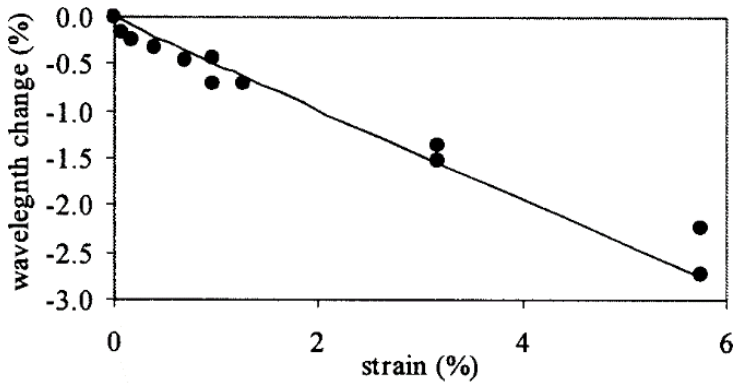

Fig. 2.15- Change in guided wavelengths for a sample of Fiber A as the strain was increased [42].

2.5 Concluding Remarks

POF based sensors are an interesting alternative to the Standard Optical Fiber sensors with their resistance to damage, their biocompatibility and the improvement of its technology over the years.

The transition of FBG and LPG based sensors to POF shows similar or better sensitivities over the Standard Optical Fibers. They show a broad application in different kinds of sensors and several types of LPG fabrication.

MPOF made the fabrication of single-mode polymer fibers possible. This allowed the fabrication of better LPGs and FBGs in polymer fibers. This type of fiber brought the possibility to create fibers with low-loss material and fewer problems with the drawing temperature. The use of MPOF presents advantages over solid-core POF, MPOFs are singlemode and composed of a single polymer allowing the fabrication of fibers with less losses.

Chapter 3
Sensors based on Fiber Bragg Gratings imprinted in polymer fibers

3.1 Introduction

Polymer fibers were first manufactured in the late 60s [9]. The main advantages of polymer fibers include larger resistance to damage and larger cores that allow better coupling [9].

FBGs are a periodic perturbation induced in the fiber with a sub-micron periodicity. This periodic perturbation reflects one wavelength denominated Bragg wavelength [14]. FBG technology have been further developed for the last three decades and has grown enough to have an important role in telecommunications [45] and optical sensing [17]. This sub-micron periodic perturbation can be achieved through phase mask technique [46] and point-by-point technique [47]. The effect of photosensitivity correlates with a permanent change in the refractive index of the fiber core when the fiber is irradiated with a UV laser. FBG inscription has already been done in polymer fibers using similar techniques as with silica fibers [48, 49]. Fiber Bragg Gratings can be written in a polymer fiber by focusing a UV laser through a phase mask in the fiber [50].

Strain, temperature and pressure sensors are very important for industrial and medical applications. The elastic properties of POFs bring advantage in strain and pressure sensing, since polymer fibers withhold more pressure and stretch further without breaking. They can be used in applications where silica fibers would break and used in medical applications due to the higher biocompatibility.

In this chapter, it is shown the setup and process for the fabrication of an FBG and the evolution of the reflection during the process of fabrication using the phase mask technique. FBGs in solid-core polymer fibers were studied as sensing elements for the measurement of strain, temperature and pressure.

3.2 FBG Fabrication

The fabrication setup is shown in Figure 3.1. An He-Cd laser that emits a 30 mW UV beam, with a wavelength of 325 nm, was used to change the refractive index of the core of the fiber. The UV beam is focused into the core of the fiber using a cylindrical lens, through a standard phase-mask with a period of 885 nm to imprint the grating.

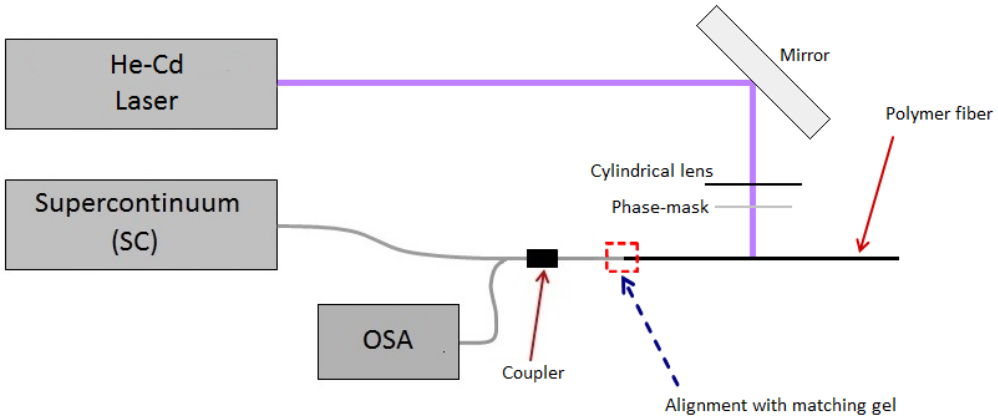

Fig. 3.1 – FBG fabrication setup.

The spectral response is observed in reflection using a 3 dB optical coupler and an Optical Spectrum Analyzer (OSA) to read the optical signal. The connection between the silica fiber and the polymer fiber were aligned using a 3D translation stage and matching gel to improve the light coupling.

Three similar polymer fibers were subjected to this inscription. The reflection spectrum was observed and timed after turning the laser on. As the grating increases, it begins to reflect a small fraction of the Bragg wavelength (Fig. 3.2). The grating first shows up with a Bragg wavelength around 1312.5 nm.

The grating then increases the amount of power that is reflected (Fig. 3.3). A shift is visible during the fabrication, This happens due to the constant change in refractive index that occurs during the irradiation process [51], and a bandwidth growth, due to power being coupled to the cladding [52]. Figure 3.4 presents the evolution of the characteristics of the FBG. Comparing all graphs, it is visible that a change in the type of the FBG happens around 4 minutes after starting the UV irradiation. The FBG has initially a narrow bandwidth and low reflectivity and it is called a type I[2] POF Bragg grating. After 4 minutes the spectrum starts to get broader, with a

[2] Type I FBG – Narrowband FBGs with low absorption and low power coupled to the cladding, meaning that the reflection compliments the transmission.

larger reflectivity while the Bragg wavelength shifts to lower wavelengths, starting to change to a type II[3] POF Bragg Wavelength [51, 52]. Figure 3.5 presents the three FBGs written. After stopping the irradiation, the fiber relaxed causing some changes to the reflection spectrum of each FBG.

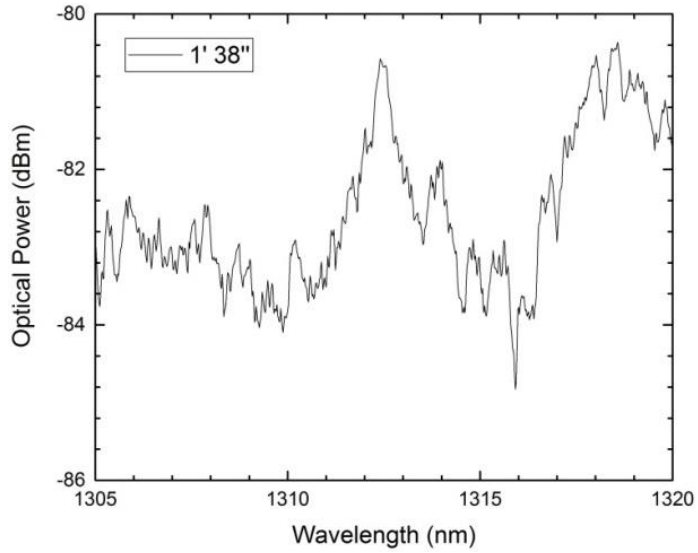

Fig. 3.2 – Small reflection appearance during inscription at 1 minute and 38 seconds.

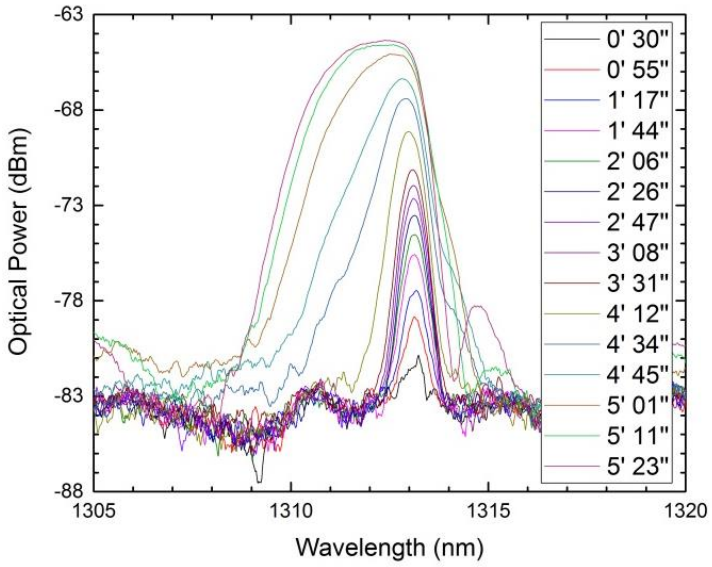

Fig. 3.3 – Reflection spectrum evolution during the FBG inscription.

[3] Type II FBG – Broadband FBGs with high reflectance and losses at lower wavelengths associated with power coupled to the cladding.

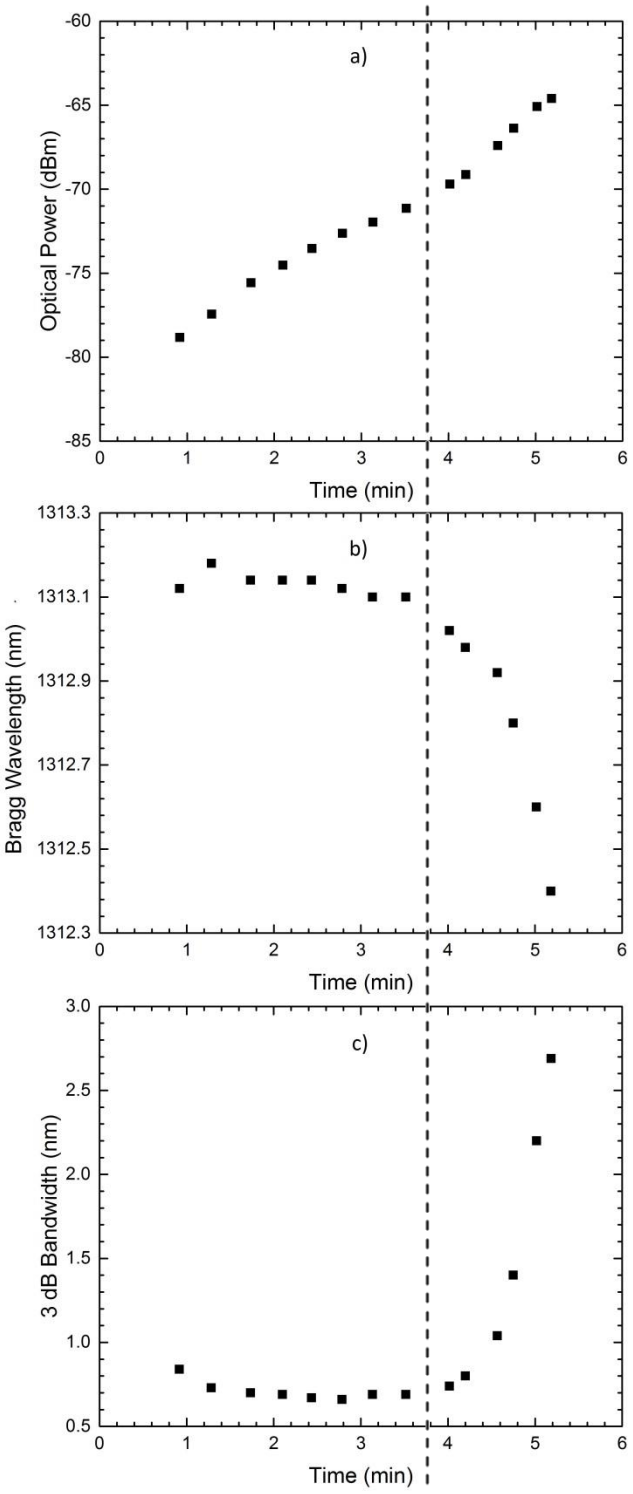

Fig. 3.4 – a) Power reflected by the FBG, b) Bragg wavelength shift and c) 3 dB bandwidth during the process of irradiation.

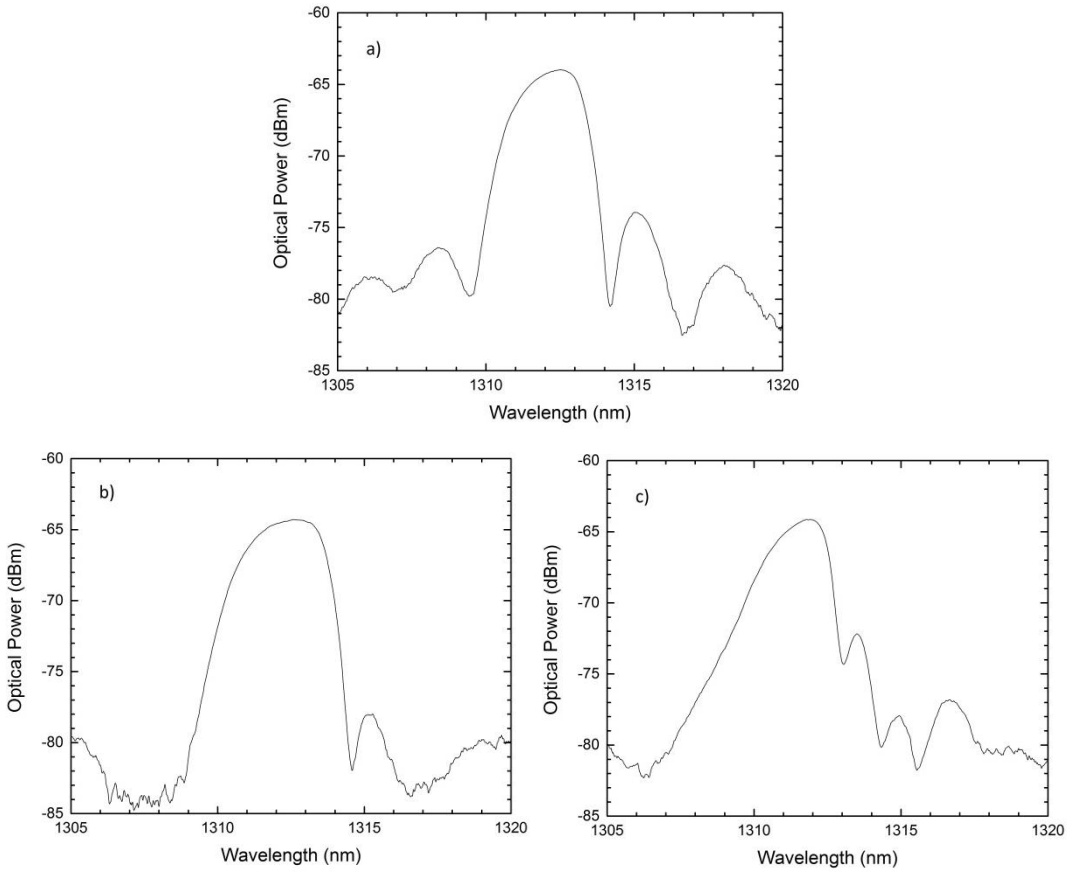

Fig. 3.5 – Spectra of the FBGs after a) 8 minutes, b) 6 minutes and 18 seconds and c) 6 minutes and 35 seconds of irradiation

3.3 Characterization and Experimental Results

Two FBGs were imprinted at Wrocław University of Science and Technology. The spectra of two FBGs were observed in reflection with the use of an optical circulator. The FBGs were characterized in strain, temperature and pressure using the configuration presented in Figure 3.6.

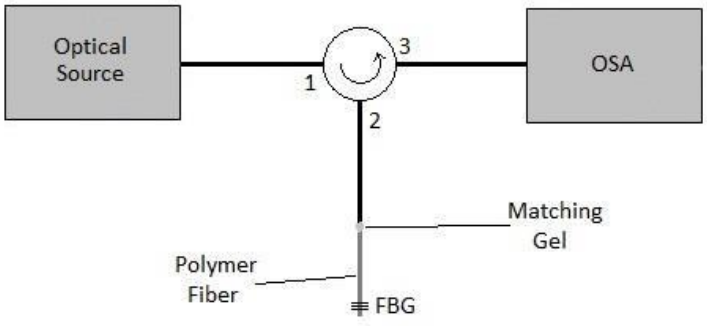

Fig. 3.6 – Experimental Setup.

In order to couple the light into the polymer fibers, a translation stage with 3 axis was used to properly align the two fibers. Matching gel was used to prevent reflections at the end face of the standard fibers that would stop light from coupling into the polymer fibers. For the strain tests, the polymer fiber was glued in two spots and stretched. The distance L between the two glued spots was measured so the strain could be measured. In order to make pressure on the FBGs, several weights, of 250 g each, were put over the FBGs. The weights were balance on top of the fibers in order to induce pressure correctly. To test the sensitivity of the FBGs to the temperature a small oven was used. The FBG was introduced in the oven, controlled by a voltage generator and the temperature was measured with a thermometer with a resolution of 0.1 ºC. The oven presented linear behavior with voltage of 8.37 ºC/V (Fig. 3.7).

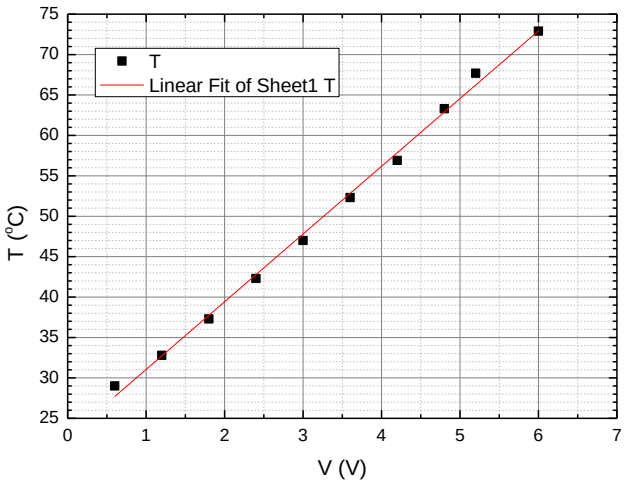

Fig. 3.7 – Thermal behavior of the oven.

A light source centered at 1300 nm and an OSA set at High sensitivity were used. The FBGs, one with a Bragg wavelength of 1312.4 nm (Fig. 3.8) and the other with a Bragg wavelength of 1312.0 nm (Fig. 3.9), were tested, both with a distance of 3 mm from the position of the FBGs to the end face of the fiber.

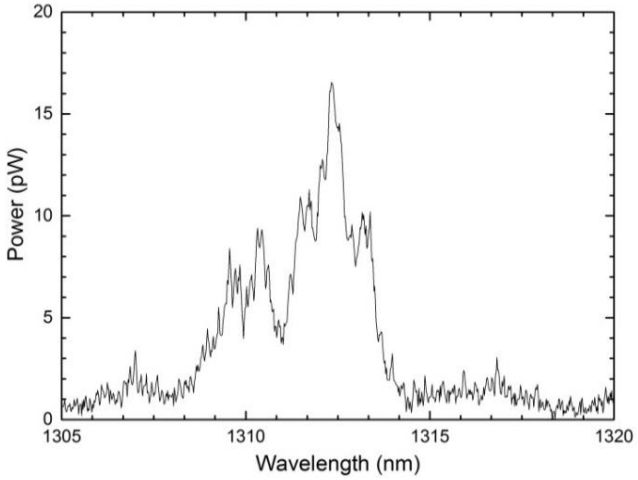

Fig. 3.8 - Spectrum of the FBG at 1312.4 nm with 0.05 nm of resolution.

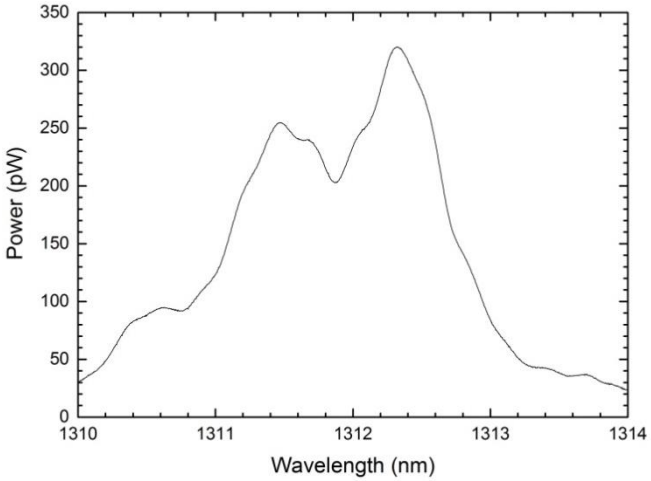

Fig. 3.9 - Spectrum of the FBG at 1311.9955 nm with 0.2 nm of resolution.

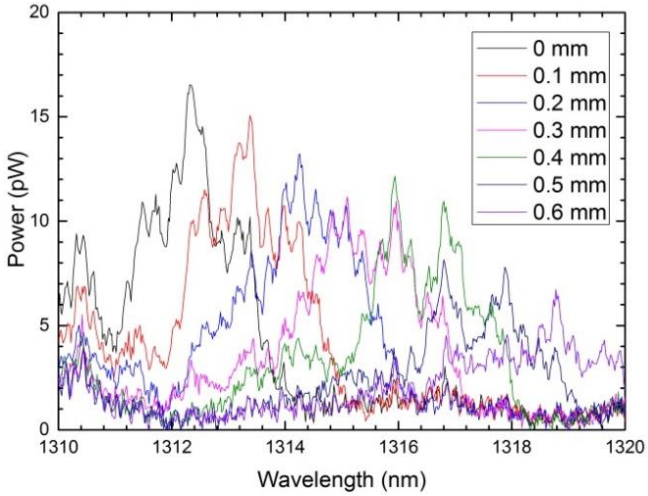

Fig. 3.10 - Bragg Wavelength shift with strain.

The first FBG was tested in strain and temperature and the second in pressure in order to analyze their response. The strain setup was used, with $L = 113\,\mathrm{mm}$

between the glued points. The fiber was stretched 0.1 mm for each measurement. In Figure 3.10 the spectra for each strain applied is displayed.

The strain applied in the fiber decreased its refractive index and increased the periodicity of the FBG resulting in a positive shift in the Bragg wavelength. This happens due to the effects of the changes in the periodicity being larger than the effects with the change in the refractive index.

To read the peaks of the reflection of the FBG, a fast Fourier transform (FFT) was used to filter the frequencies of the oscillation. A strain sensitivity of $1.91 \pm 0.5\ \mathrm{pm}/\mu\varepsilon$ was obtained through a linear fit.

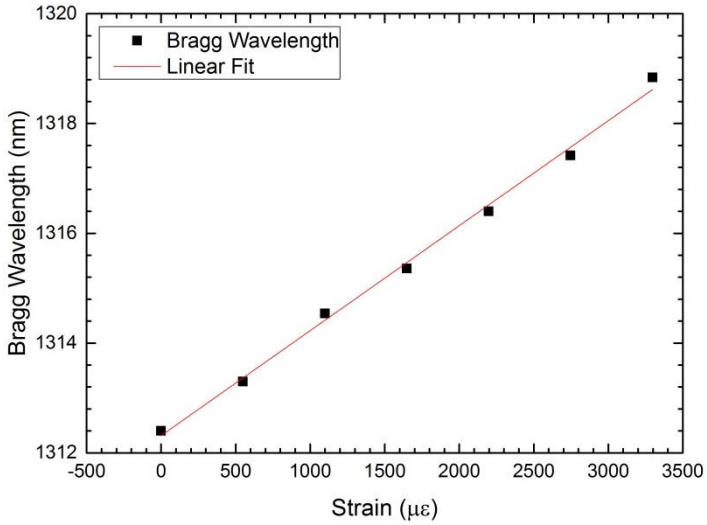

Fig. 3.11 - Sensitivity to strain.

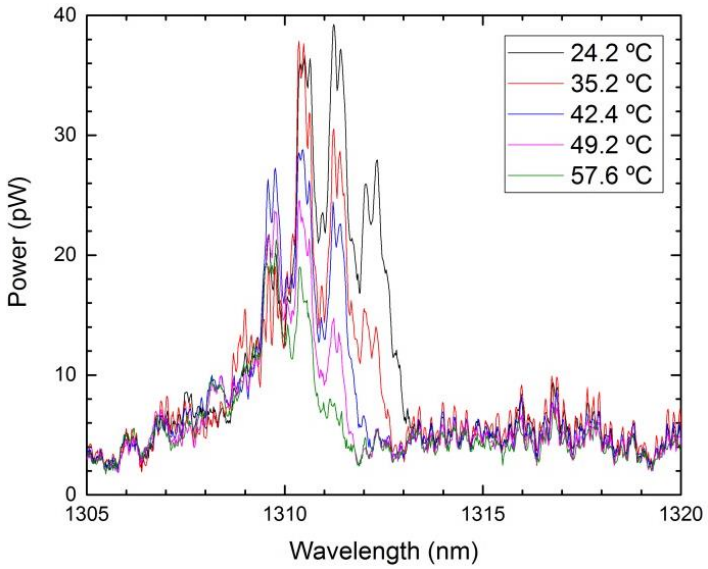

Fig. 3.12 - Spectrum variation with temperature.

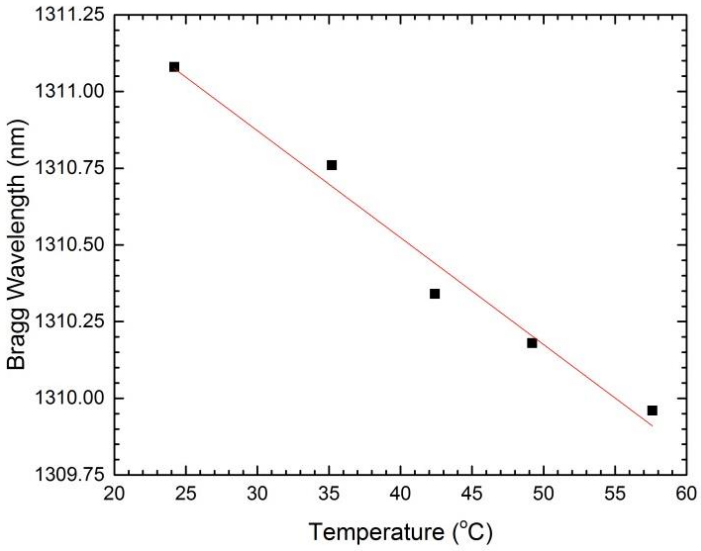

Fig. 3.13 - Temperature sensitivity.

The fiber was inserted in the oven with no curvature nor strain applied. Using the oven, the effects of the temperature to the FBGs were observed in the spectra. In Figure 3.13, a negative shift with the increase of the temperature.

Thermo optical effects decrease the refractive index of the fiber while the fiber expands with the heat. The negative slope is due to the thermo optical effects in the fiber that are larger than the fiber expansion effects, shifting the Bragg wavelength to smaller values. Through a linear fit, the sensitivity obtained was $-35 \pm 3\ \mathrm{pm/°C}$. This happens due to thermo-optical effects in PMMA where the refractive index decreases with the increase of the temperature [53]. Unlike silica fibers, polymer fibers present a negative sensitivity due to the different material composition, that present different thermo optical effects. Although the range for the temperature sensor is smaller than FBG based sensors in silica fibers, the characteristics of polymer fibers make the sensor more sensitive than in the silica counterpart.

For pressure tests, weights were stacked on top of the second FBG. The weights were balanced on top of the fiber to avoid tilting and so the area of contact is always the same. For each weight, a spectrum was attained from the OSA (Fig. 3.14). The sensitivity of the FBG to pressure, presented in Figure 3.15, exhibits an increasing non-linear behavior.

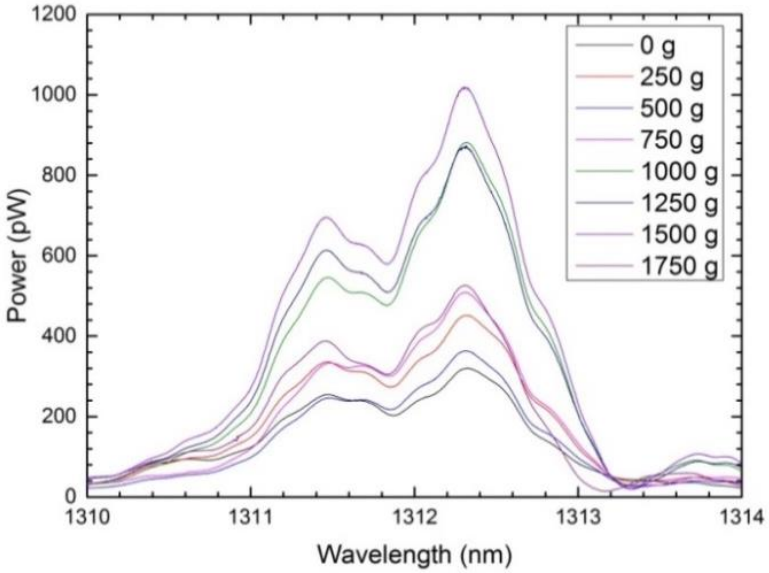

Fig. 3.14 - Spectra variation with pressure.

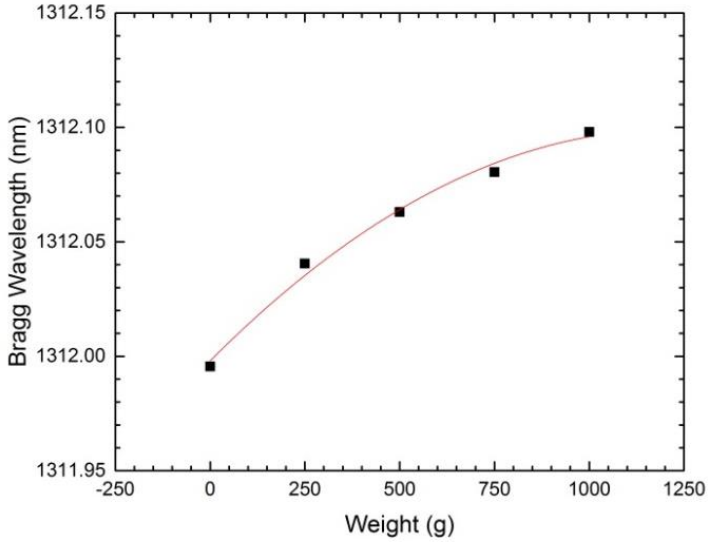

Fig. 3.15 - Pressure sensitivity.

The pressure applied in the fiber induces a fiber strain decreasing its refractive index and increased the periodicity of the FBG causing a positive shift in the Bragg wavelength. This effect is similar to applied longitudinal where the effects of the changes in the periodicity are also larger than the effects with the change in the refractive index.

3.4 Conclusion

Three FBGs were imprinted in polymer fibers using the phase-mask technique. It was observed that the characteristics of the FBG start to differ after maintaining the UV irradiation for some time. At first the power of the FBG increases quickly but at a certain point in time the rate decreases and the bandwidth begins to increase.

The FBGs in polymer fiber exhibit sensitivity to strain, temperature and pressure. The strain sensitivity obtained was $1{,}91 \pm 0.5\ \mathrm{pm}/\mu\varepsilon$ and the temperature sensitivity was $-35 \pm 3\ \mathrm{pm}/°\mathrm{C}$. There was a small positive non-linear shift of the Bragg Wavelength with the increase of pressure.

Chapter 4
Fabry-Perot cavity based on FBGs in Polymer Fiber for refractive index measurement

4.1 Introduction

Refractive index measurements of liquid substances are important for several applications in medicine, biology and chemistry. Abbe refractometers are used to measure refractive index through the detection of the critical angle [54]. These refractometers are often large and not very practical for medical and biological applications as they require certain measurement conditions like the use and disposal of part of the sample. Fiber optic based sensors proved to be an alternative solution due to their small size, high sensitivity and other characteristics like biocompatibility, making them good for minimal invasive measurements. Most often their operation principle is based on the analysis of changes in the spectrum caused by a specific parameter change. For measuring refractive index the use of birefringent fibers [55–57], fiber gratings [8, 55, 56, 58–60], optical fiber coatings [61, 62] and fiber interferometers [55, 57, 58, 63] are presented in literature.

Among different fiber refractometer concepts, the surface plasmon resonance based devices allow for achieving particularly high measurement resolution, reaching 10^{-7} RIU [62]. Recently, it has been demonstrated [63] that using two micromachined Fabry-Perot cavities at the tip of the fiber similar resolution are achievable, however, manufacturing of such a sensor required multistep, complex procedure.

In spite of lower measurement resolution, fiber Bragg gratings [45] offer several advantages in refractive index sensing. Small sizes as well as the possibility of reflection interrogation and wavelength multiplexing are some of them. It has been shown [59] that FBGs written in suspended core fibers allow for measuring the refractive index change as small as 3×10^{-5} RIU. Lower resolution of 3×10^{-3} RIU has been achieved by using an FBG written in H-shaped fiber [56], however, this solution made it easier for accessing the evanescent optical field and thus allowed for much faster measurements. Similar resolution of 5.5×10^{-3} RIU and possibility of improvement up to 5×10^{-5} RIU have been reported by using FBGs written in exposed-core microstructured optical fibers [60]. On the other hand it is convenient to combine

the FBG with a fiber tip where light reflects many times between the grating and the fiber end-face, thus creating Fabry-Perot cavity. The visibility of fringe pattern depends on the Fresnel reflection at the fiber end-face, therefore by dipping the tip of the fiber in a liquid one can measure its refractive index. This kind of sensor is easy to fabricate and allows for fast and simple operation. By now, refractometers of this design were reported for silica fibers [55, 58] yielding a sensitivity ranging from $-1.06\ \mathrm{RIU}^{-1}$ to $-3\ \mathrm{RIU}^{-1}$ and the resolution of $10^{-3}\ \mathrm{RIU}$.

The first FBGs in POFs were fabricated in late 1990s [50] and since that such structures have been gaining attention [52, 64]. In this chapter, the use of FBG based Fabry-Perot cavity in POF for refractive index measurements was investigated. The measurement method proposed was similar to previous studies in silica fibers [55], [58]. However, using POFs for sensors fabrication opens new application opportunities in medicine and biology due to better biocompatibility of polymer fibers. Moreover, the use of polymer fibers eliminates a practical limitation of sensors based on silica fibers related to fragility of the fiber tip which might get damaged during sensing procedure.

4.2 Experimental Setup

The setup used in the experiment is shown in Figure 4.1. A supercontinuum (SC) was used as a light source and the reflection spectrum of the interferometer was observed in the OSA. The POF was a $268\ \mu\mathrm{m}$ diameter solid core fiber with a $3.8\ \mu\mathrm{m}$ diameter core. The fiber was composed of PMMA in the cladding and a copolymer of PMMA and polystyrene in the core ($5\ \mathrm{w/w\%}$). The connection between the silica fiber and the POF required alignment and matching gel in order to couple the light into the core and avoid creating a cavity between both fibers.

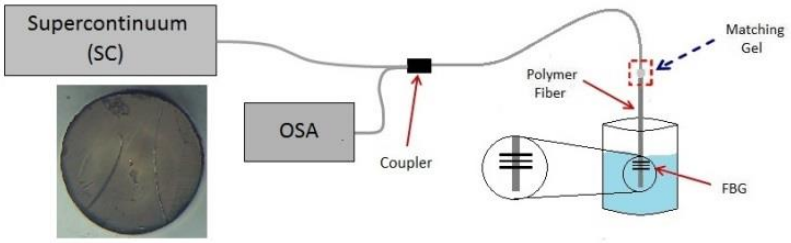

Fig. 4.1 – Experimental setup for characterization of the Fabry-Perot interferometer based sensor. On the inset a cross section of the POF is shown.

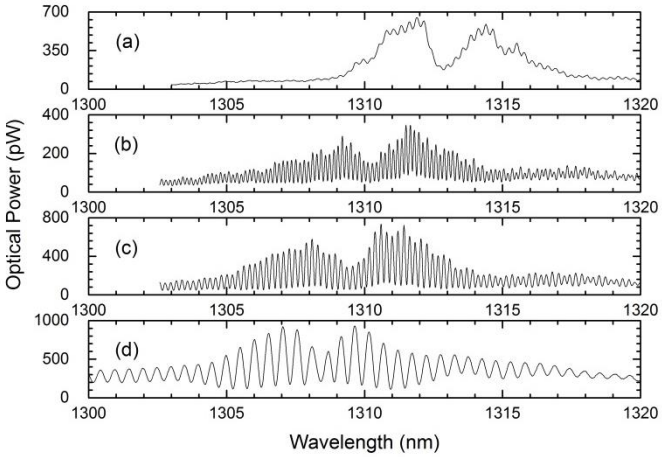

Fig. 4.2 – (a) Reflection spectrum of the FBG before making a cavity. (b) Reflection spectrum with a cavity length equal to 3.6 mm, (c) 2.8 mm, (d) 1.1 mm recorded in air.

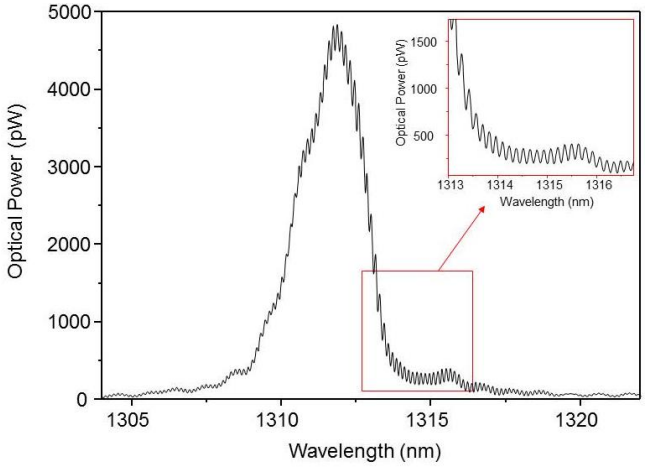

Fig. 4.3 - Reflection spectrum of a Fabry-Perot interferometer formed by an FBG and fiber end face recorded in air. The FBG exhibits higher reflectance than the one in Fig. 4.2.

A UV laser beam ($\lambda = 325\ \mathrm{nm}$) was focused on the fiber through a cylindrical lens and a phase mask [50, 52, 64] to write the FBG. In the reflection spectrum of the fabricated FBG two peaks were visible. The peak splitting appears most likely because the POF has not been annealed prior to the grating inscription. As it was shown in paper [52], in such a case, a spectrum of an FBG may get distorted after some irradiation time. This effect originates from temperature increase occurring in POFs when exposed to the UV which results in random grating shrinkage due to stress relaxation and affects the reflection spectrum.

The fiber was cleaved in close distance to the grating. As the light was reflected back and forward between the FBG and the end of the fiber, a cavity was formed and a fringe pattern appeared on the reflection spectrum of the FBG. A spectral separation of adjacent interference fringes observed in the reflected spectrum can be expressed as $\Delta\lambda = \lambda_0/2nl$, where *n* is the effective refractive index of the core, *l* is the length of the

cavity and λ_0 is the central wavelength of the fringe pattern. Figure 4.2 shows the fringe pattern for different cavity lengths (the fiber was cut several times). During each cutting procedure the fiber tip was annealed in the cutting board which shifted the spectrum (the temperature of the cutting board was about 73°C). In its final shape the spectrum consisted of the fringes of the periodicity $\Delta\lambda$ equal to 0.51 nm which corresponds to a cavity length of 1.1 mm (Fig. 4.2). The fringe visibility was equal to 68% which means that the optical power reflected by the FBG and the end-face of POF does not differ significantly. Therefore, reflectance of the grating was close to 4%, which is due to long irradiation time used in fabrication of the FBG. For comparison, another grating with much higher reflectance was fabricated and a FP cavity was formed again. It can be seen in Figure 4.3 that the fringe visibility in this case was much lower (4%).

4.3 Results

Glycerin solutions in water of different concentrations were prepared to test the performance of the sensor. The values of the refractive index of the liquids ranging from 1.33800 to 1.47650 were first measured with an Abbe refractometer. Around 15 mm of tip of the fiber were dipped into every liquid and the spectrum acquisition was done during a 15 seconds period. Therefore, short time required for obtaining the result was one of the advantages of the presented setup. In Figure 4.4 it is visible that the average power and the contrast of interference fringes were dropping with the increase of the refractive index. The spectra were analyzed using a fast Fourier transform to obtain the amplitude of the frequency of the fringes (Fig. 4.5). In order to avoid problems with the power source or any other instability during the measurements, the amplitude was normalized with respect to the amplitude of the fringes in air, registered prior to each measurement of liquid with different refractive index. For the normalized amplitude a linear behavior was observed against refractive index changes (Fig. 4.6). A sensitivity of $-1.94\ \mathrm{RIU}^{-1}$ was obtained with this sensor. Ten measurements of the same liquid were done and the scattering of the results was 0.0018 which is shown on the inset of the Figure 4.6. Therefore, the estimated measurement resolution of the sensor is equal to $1 \times 10^{-3}\ \mathrm{RIU}$.

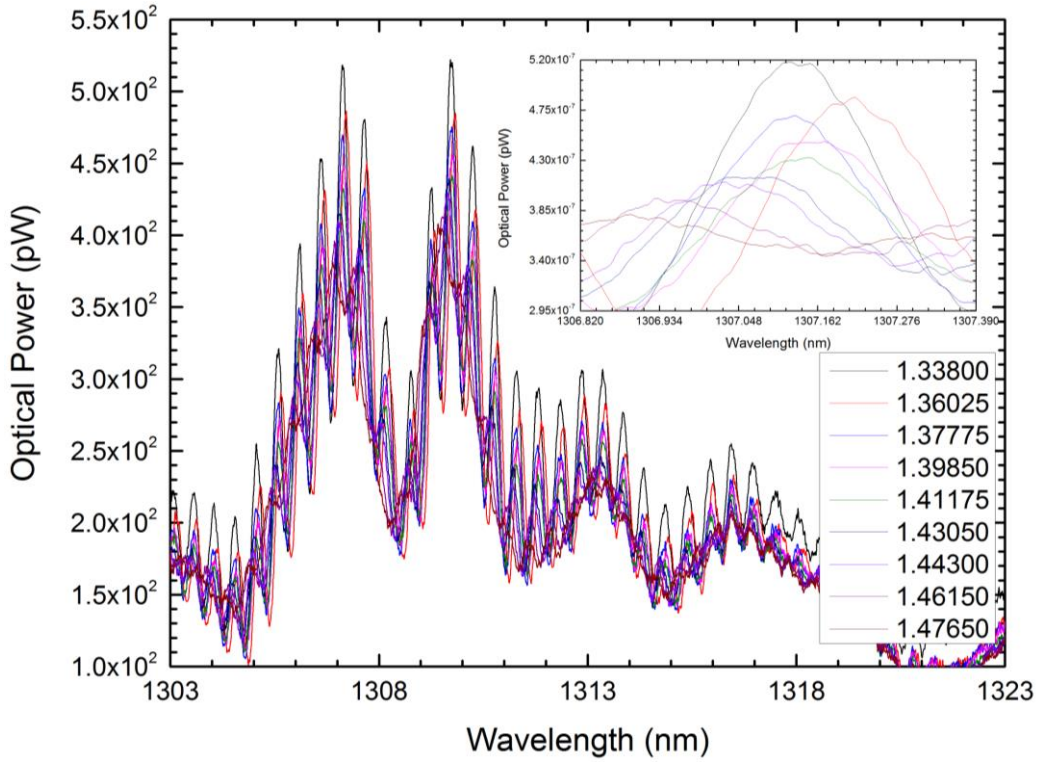

Fig. 4.4 – Reflection spectra of a FP cavity for different refractive indices, the contrast of interference fringes drops with increasing refractive index.

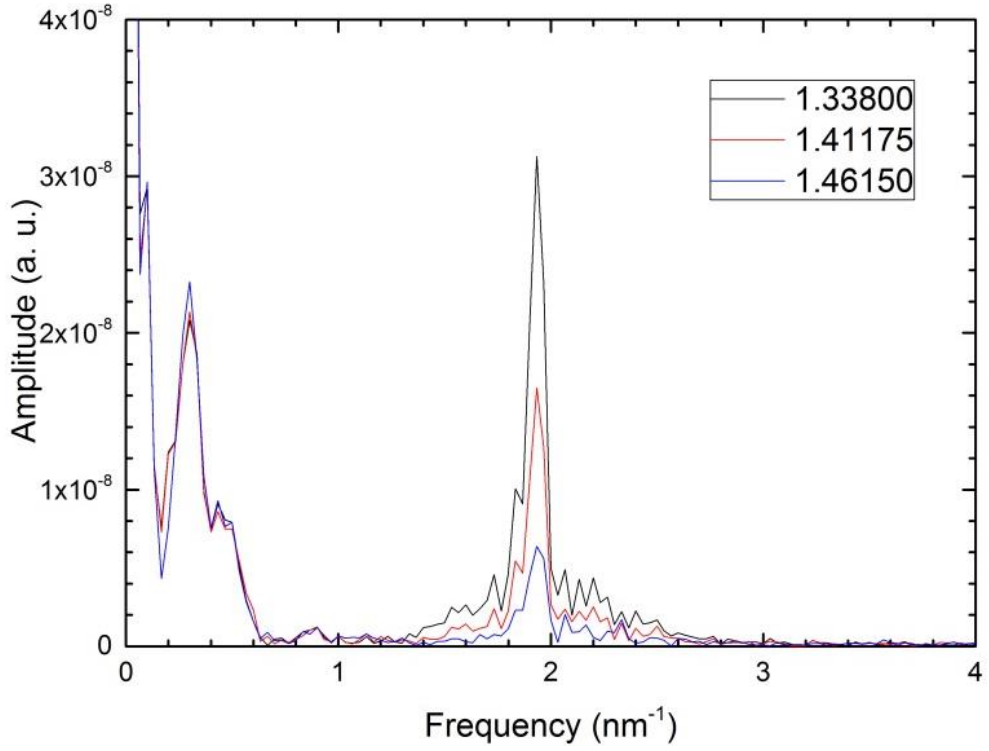

Fig. 4.5 – FFTs of the reflection spectra for 3 liquids with refractive indices of 1.33800, 1.41175 and 1.46150.

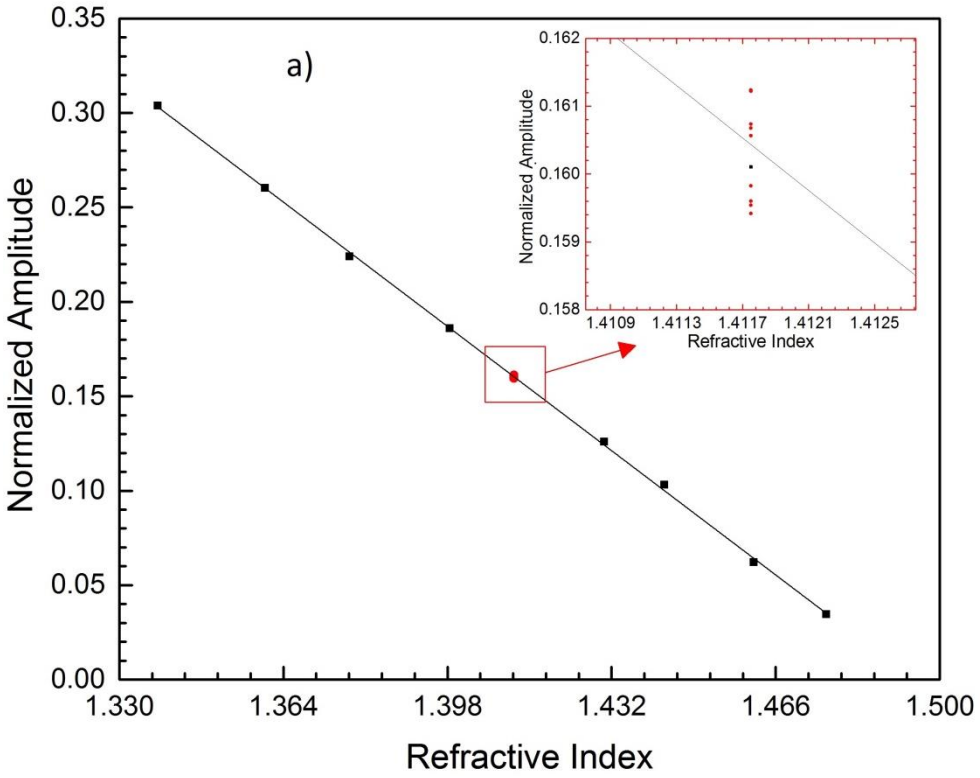

Fig. 4.6 – Dependence of normalized amplitude of the frequency of the interference fringes upon refractive index changes.

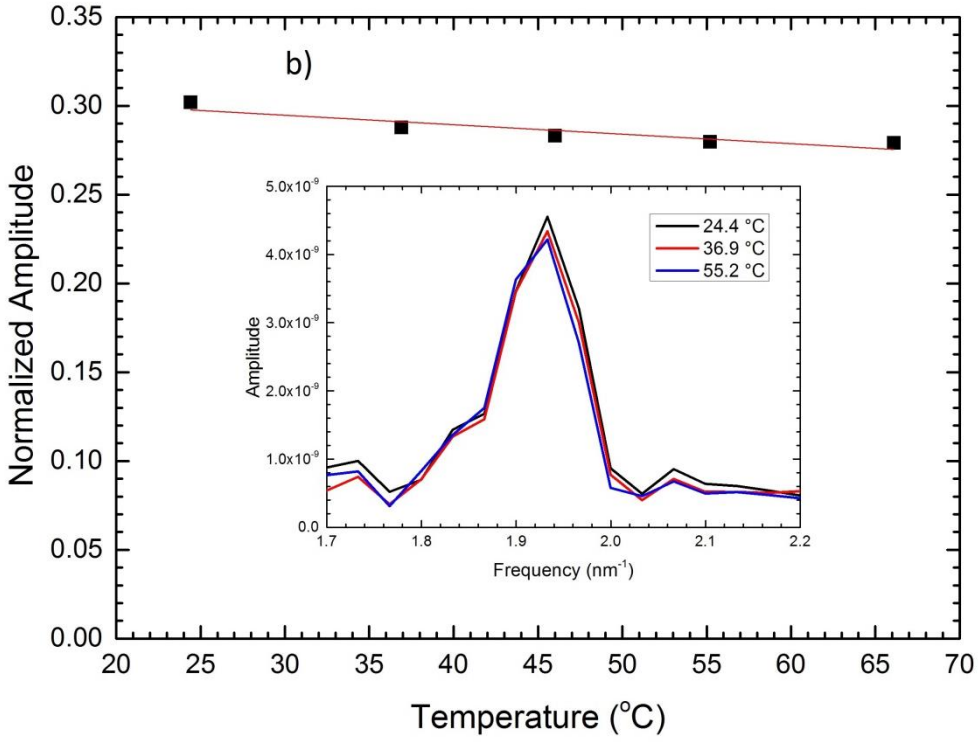

Fig. 4.7 – FFTs of the spectra at different temperatures. The normalized amplitude of the peak frequency of the fringes drops with the increase of the temperature.

Moreover, the sensor was tested for temperature response in the range of 24.4 to 66.1 °C. The FFT was used to analyze the reflection spectrum (Fig. 4.7), achieving a

low sensitivity of $-5 \times 10^{-4}\ °C^{-1}$. This behavior implies that the difference between the refractive indexes of the polymer fiber and the water decreases with the increase of temperature. Since both values drop with temperature in the examined range [65, 66], the refractive index for polymer fiber drops faster than the one for water. It is important to calculate the ratio between the temperature and the refractive index sensitivities, also known as cross sensitivity. A cross sensitivity of $3 \times 10^{-4}\ \mathrm{RIU}/°C$ was attained. For small temperature deviations the sensor can read up to 3 decimal cases.

4.4 Conclusion

In this chapter, the possibility of using POFs for refractive index measurements of liquids was demonstrated. The sensor proved to be capable of measuring the refractive index with a resolution of $1 \times 10^{-3}\ \mathrm{RIU}$. The results were reproducible and a refractive index sensitivity of $-1.94\ \mathrm{RIU}^{-1}$ was obtained in a range from 1.33800 to 1.47650. It is worth to emphasize that the presented setup allowed fast measurements. Moreover, the use of POFs makes the sensor more biocompatible and eliminates the problem of tip fragility limiting the applications of silica fibers based sensors of this type.

Chapter 5

Polymer fiber imprinted LPG based sensors

5.1 Introduction

LPGs are nowadays an interesting tool to create sensors. Several silica LPG based sensors were fabricated in the past [25–27].

The use POF for making LPG based sensors can bring the advantages of polymer fibers to create new sensors. This combination was already fruitful and brought the creation of different sensors [35, 37, 38].

Generally, LPGs can be written in polymer fibers using mechanical imprinting or by UV writing. The point-by-point technique provides control over the all the parameters of the grating. However, PMMA has a poor photosensitivity to UV radiation [67], but this can be compensated by diffusing azobenzene into the fiber [36].

Mechanical techniques require exerting periodic pressure on the fiber. Pressure alters the refractive index locally and this allows the creation of a periodic perturbation. The use of a simple mechanical technique will only create a temporary LPG, as soon as the pressure is removed the LPG ceases to exist. To surpass this problem, the pressure points can be heated up to higher temperatures imprinting the LPGs permanently.

In this chapter, it is presented the fabrication process of fabricating LPGs using the point-by-point technique, the mechanical technique and the development of an LPG based Mach-Zehnder interferometer tested in strain.

5.2 LPG Fabrication using point-by-point technique

A 30 mW He-Cd laser, with a wavelength of 325 nm, was used to create the perturbations in the fiber. In order to have good symmetry, the beam was splitted in two to focus on both side of the fiber. To make each point, a translation stage was used to have precise translation of the fiber and create the most exact period possible for the LPG. The alignment between the silica and polymer fiber was done by focusing the light from one fiber to the other with the help of microscope lenses (Fig. 5.1).

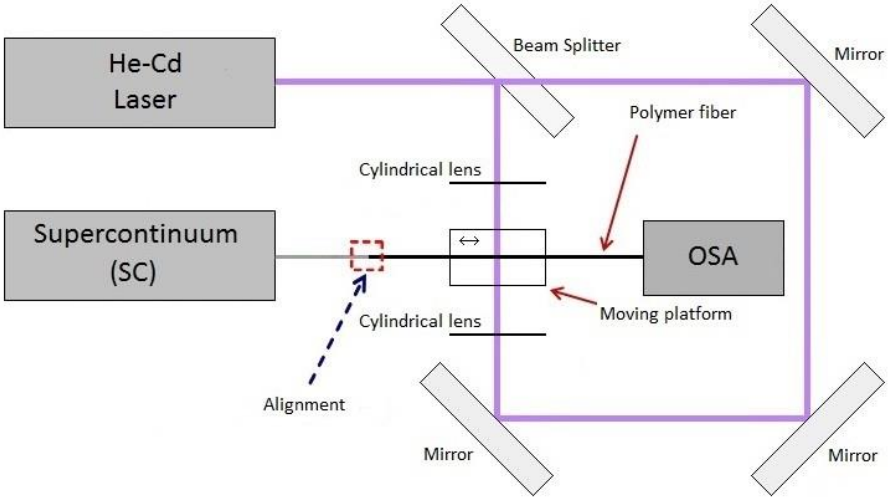

Fig. 5.1 – LPG fabrication setup.

In the fabrication process, the spectrum was being monitored as the points were being imprinted in the fiber using a transmission setup.

The limited response to UV radiation can be overcome by doping the inscribing area with azobenzene. The fiber was dipped in azobenzene and then covered to avoid evaporation. The diffusion process was carried out for around 15 minutes to have a proper doping.

The fiber was then placed in the moving platform with a camera view to observe if the UV beam was aimed correctly to the fiber. A filter was used to reduce the power of the beam to visualize where the fiber would be affected. After the alignment, the filter was removed and, for each point, the fiber was irradiated for 20 seconds and the spectrum was recorded (Fig. 5.2). The fiber was translated 1.2 mm after each point using the platform in order to have the desired periodicity.

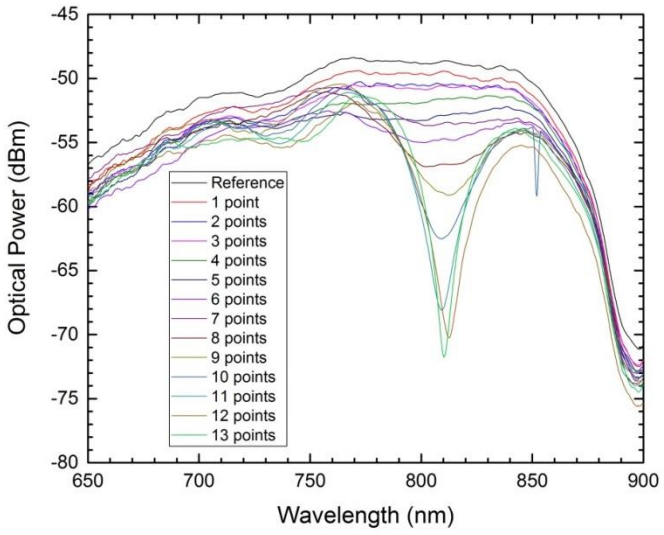

Fig. 5.2 – Evolution of the FBG after each point.

As the number of points increased the strength of the LPG increased and it got narrower. Nevertheless, the increase of the number of points will reach a threshold, after a certain amount, the LPG will have a broader spectrum and less strength for each extra point.

5.3 Sensor based on a Mach-Zehnder interferometer with two mechanically imprinted LPGs in a polymer fiber

5.3.1 Fabrication of the interferometer

In this experiment, a double LPG based Mach-Zehnder interferometer was created and tested as a strain sensor. The LPGs are imprinted in the fiber using a high temperature mechanical technique.

The setup for fabricating the interferometer is in Figure 5.3. The fiber is placed on top of a plate with periodic grooves with a spacing around 1 mm, that creates the perturbations necessary for the LPGs. Two sections of the fiber were placed on the top of the grooves and pressed with loads against them. Between the two sections there is a gap of 30 to 40 mm. The polymer fiber is in a standard transmission setup, using a supercontinuum as an optical source, so the spectrum is monitored. By tilting the fiber on top of the grooved plate, higher periodicities are achieved. With this in mind, temporary LPGs can be created to check the best period to fabricate the interferometer by observing the spectrum. Upon having the adequate period, a peltier is used to increase the temperature of the grooved plate to around 70 °C. To increase the efficiency of the process extra pressure is added on top of the fiber leaving a better perturbation on the fiber.

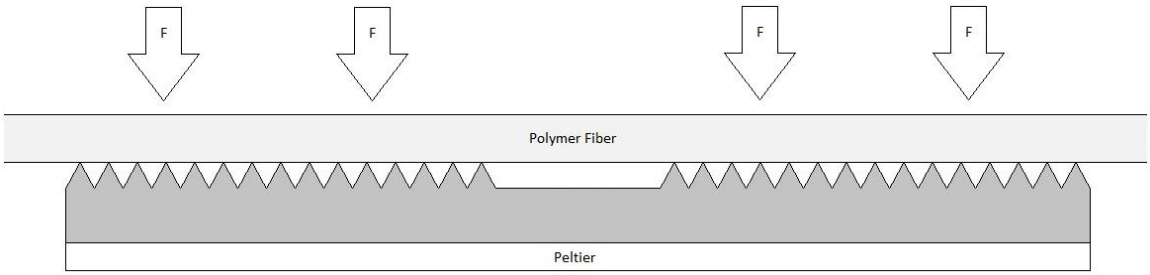

Fig. 5.3 – Interferometer fabrication.

After 7 to 10 minutes at high temperatures, the fiber was left cooling and at room temperature the loads were removed. The spectrum of the interferometer is observed by transmission. Figure 5.4 presents two interferometers fabricated.

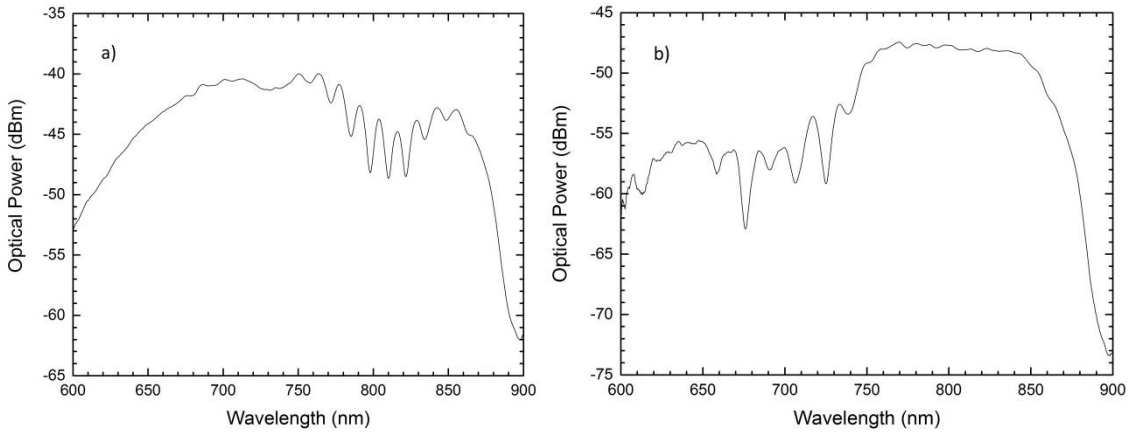

Fig. 5.4 – Spectra of two LPG based Mach-Zehnder Interferometers.

5.3.2 Strain sensor

After 25 days the interferometer from Figure 5.4 a) was tested in strain. This has given the FBGs time to stabilize so the spectrum was analyzed (Fig. 5.5).

For the strain test, a standard transmission setup was used. Only one of the LPGs was stretched. With a distance between the glued points of the fiber equal to 600 mm, the fiber was stretched 0.1 mm between each spectrum acquisition. Figure 5.6 shows a negative shift with the increase of the strain.

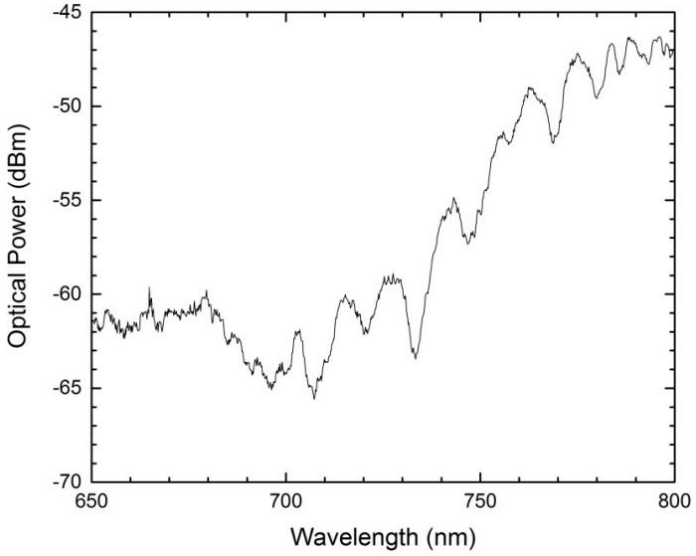

Fig. 5.5 – Spectrum of the relaxed interferometer.

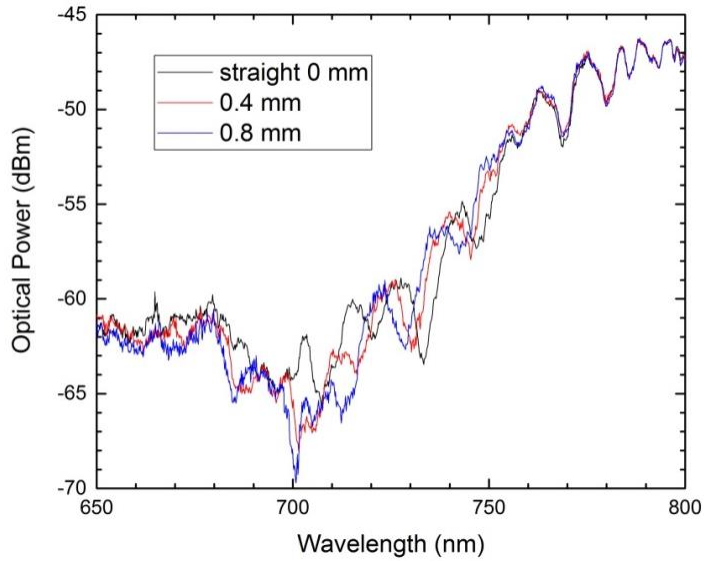

Fig. 5.6 – Spectrum shift with strain.

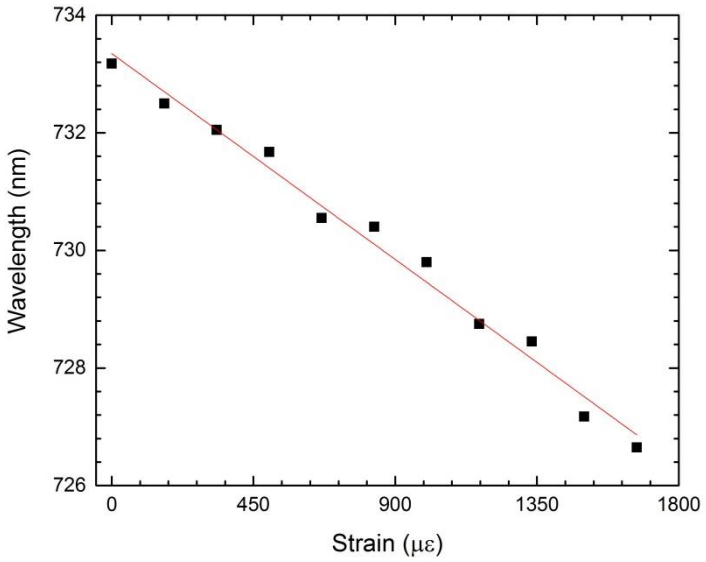

Fig. 5.7 - Strain sensitivity.

The spectra were filtered to remove noise and the position of the minimum between 740 and 750 nm was tracked (Fig. 5.7). A strain sensitivity of $-(3.9 \pm 0.2) \times 10^{-3}$ $\mathrm{nm}/\mu\varepsilon$ was obtained for the interferometer.

5.3.3 Conclusion

An LPG was written in a polymer fiber using a point-by-point technique. The device presented a narrow peak which makes viable to characterize it as a sensor by

tracking the shift of the wavelength of the peak. The evolution of the fabrication is monitored during the entire process.

An LPG based Mach-Zehnder interferometer was fabricated. The mechanical technique allowed some degree of control over the final result. The process of fabrication can be improved, but it is reliable enough to fabricate similar sensors. The sensor was tested in strain and achieved a sensitivity of $-3.9 \pm 0.2\,\mathrm{pm}/\mu\varepsilon$. The negative sensitivity is due to elasto optic effects in the polymer fiber.

Conclusion and Future Work

In this dissertation, the fabrication and characterization of optical sensors was based on POF presented. These sensors were based either on fiber Bragg grating and long period gratings.

FBGs were imprinted in polymer fibers. These devices showed potential for optical sensing applications. The FBG based sensors were characterized for strain, temperature and pressure by tracking Bragg wavelength shifts. The achieved sensitivities were $1.91 \pm 0.5\ \mathrm{pm}/\mu\varepsilon$ for strain, $-35 \pm 3\ \mathrm{pm}/^{\circ}\mathrm{C}$ for temperature and a positive non-linear sensitivity for pressure.

A Fabry-Perot interferometer was developed by making a cavity between an FBG and the end of the fiber. The sensor was characterized for refractive index achieving a sensitivity of $-1.94\ \mathrm{RIU}^{-1}$ with a cross sensitivity of $3 \times 10^{-4}\ \mathrm{RIU}/^{\circ}\mathrm{C}$.

Two types of LPG imprinted were studied. Point-by-point inscription allows the control of the parameters of the LPG and the observation of the evolution of the LPG. Mechanical imprinting can either create temporary or permanent LPGs and gives an insight of what the chosen parameters achieve before permanently imprinting the LPGs. This technique also gave the opportunity of easily developing an LPG based Mach-Zehnder interferometer that presented a strain sensitivity of $-3.9 \pm 0.2\ \mathrm{pm}/\mu\varepsilon$.

The work here presented in this dissertation could be improved and further investigated. It is proposed:

- Combining FBG based sensors with 3D printing technology for pressure sensing.
- Improving the quality of LPG based Mach-Zehnder interferometers and find new applications for the improved version.
- Investigate the possibility of polymer fiber for humidity sensing.

Appendix I

Cutting Machine development

Polymer fibers are structurally different from silica fibers. In order to cut silica fibers, a cutting machine with a blade is used. Due to the characteristics of POF, this machine does not work for cutting them, neither using x-acto knives. In order to cut polymer fibers, a higher temperature than the room temperature is necessary, a sharp blade and a precise transversal cut. The higher temperature reduces the strength needed to cut the fiber thus avoiding fiber bending during the cut.

I.1. Background

Wrocław University of Science of Technology possessed a cutting machine seen in Figure I.1.

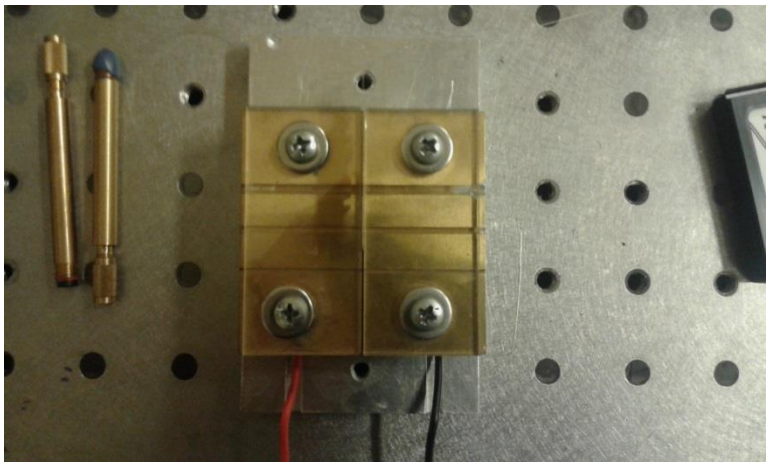

Fig. I.1 - Polymer Fiber Cutting board owned by Wrocław University of Science and Technology.

The machine is composed of two brass plates with slits where the fiber can fit and a hole to introduce the thermometer, a protective layer made of two pieces of acrylic, a peltier for temperature increase and a shaving blade. The peltier sits on an aluminum plate with termal paste. The peltier is then connected to a voltage or current generator.

The cut is at its best at a temperature that rounds 73 °C. The shaving blade slides in between the two brass plates to make the cut.

I.2. Reproduction

To build a similar cutting board, a 3D drawing was made using the program *AutoCAD*. The peltier and from the thermometer were measured to adequate the machine to it and to hold some improvements. The drawing was divided in four parts, two aluminum parts, the brass part and the acrylic one.

I.2.1. Base for the peltier

The base of the machine with a cavity for the peltier was planned to be made of aluminum. The cavity was drawn slightly larger than the peltier dimensions and tracks for the wires of the peltier were added to avoid damage during the heating. Figures I.2 and I.3 present the drawings in two perspectives with the distances and sizes presented in mm.

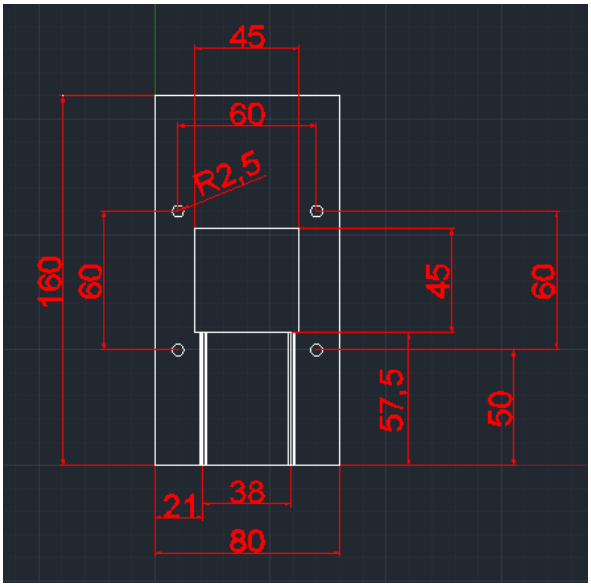

Fig. I.2 - Top view of the base, values in mm.

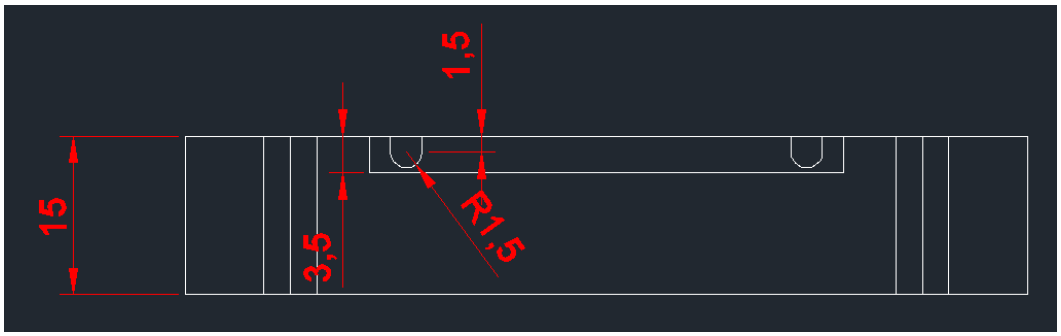

Fig. I.3 - Front view of the base, values in mm.

Holes for the screws were also planned which would vary depending on the size of the used screws. They were meant to attach the cover on top of the base.

I.2.2. Aluminum cover

An aluminum cover was designed as an interface between the base and the tracks. This cover protects the peltier from the shaving blade. Figures I.4 and I.5 present two perspectives of the plate.

The cover connects to the base and to the plate with the tracks. The screws from the plate with the tracks can't go below the cover, but the size of the hole may vary depending on the chosen screws.

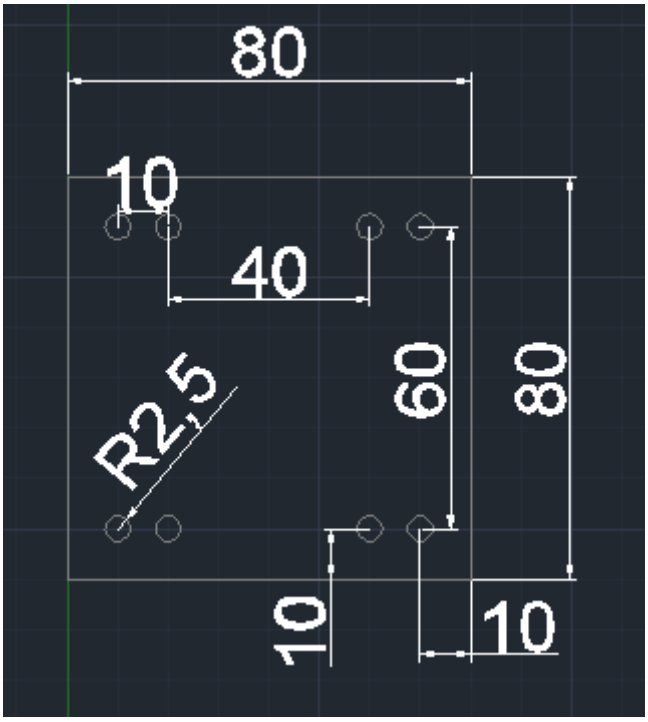

Fig. I.4 - Top view of the cover plate, values in mm.

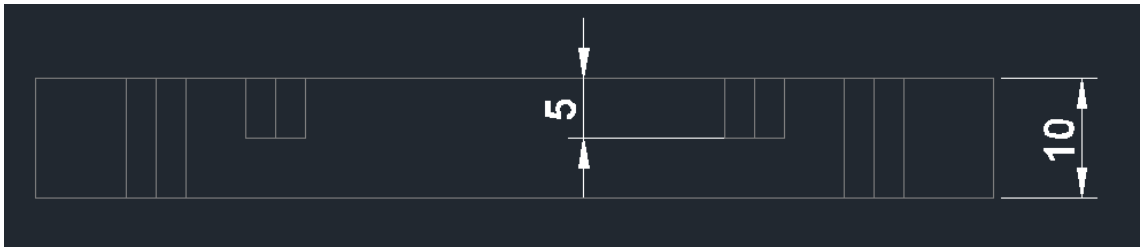

Fig. I.5 - Front view of the cover plate, values in mm.

I.2.3. Brass fiber tracks and thermometer hole

These plates contain the tracks for the fiber and a hole for the thermometer. A separation is left between the two plates large enough to the sliding the blade. The tracks are larger than polymer fibers, but small enough for the fiber to stay stretched in it. Two views are presented in Figures I.6 and I.7. The screw holes were made larger so it was possible to adjust the distance between both brass plates in order to make the best possible cut.

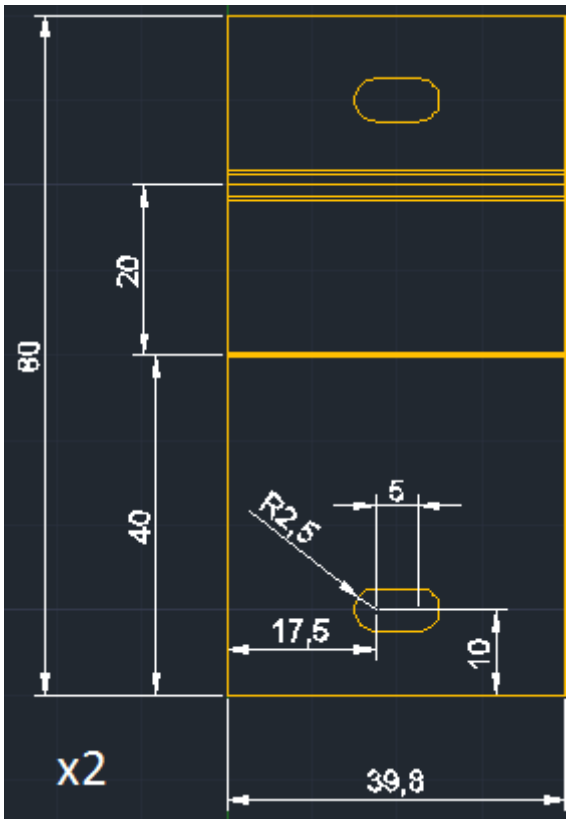

Fig. I.6 - Top view of one of the brass plates, values in mm.

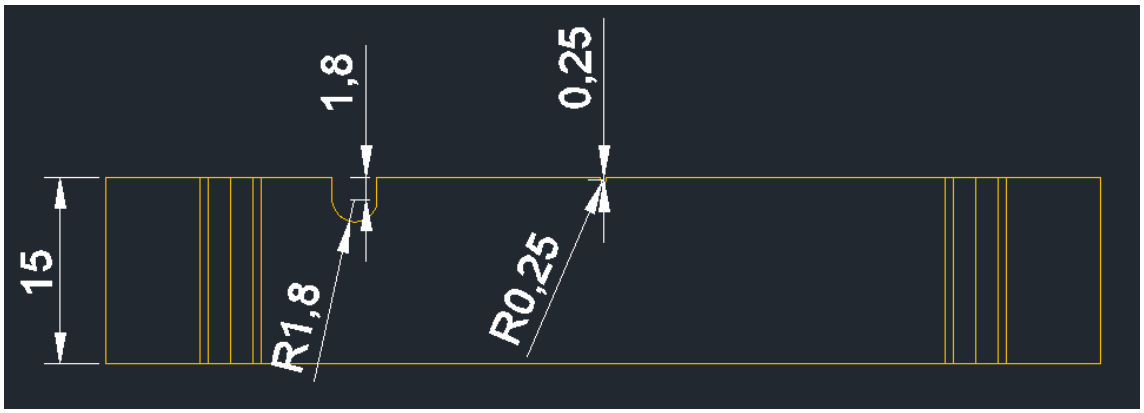

Fig. I.7 - Side view of the brass plates, values in mm.

I.2.4. Acrylic protection

The protection was composed of two pieces made of acrylic to protect the user from getting burned. Besides protection, the plates also hold the fibers on the track preventing any bend. Two perspectives of the acrylic plates can be seen in Figures I.8 and I.9. The screw hole needed the same functionality as the ones in the brass plates thus they were made larger.

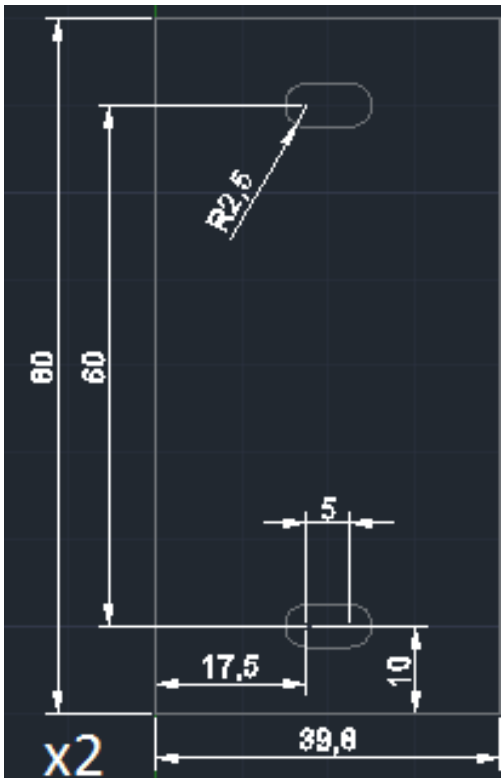

Fig. I.8 - Top view of both acrylic plates, values in mm.

Fig. I.9 - Front view of on acrylic plate, values in mm.

I.3. Results

With every piece drawn, the final sketch of the cutting machine can be seen in Figure I.10.

The drawings were sent to the workshop where every plate was carved. Figure I.11 shows the new cutting machine after placing the peltier and assembling the pieces.

In Figure I.12, a cut is displayed. The core is emitting a symmetrical beam, showing that it's a proper cut to align the fiber.

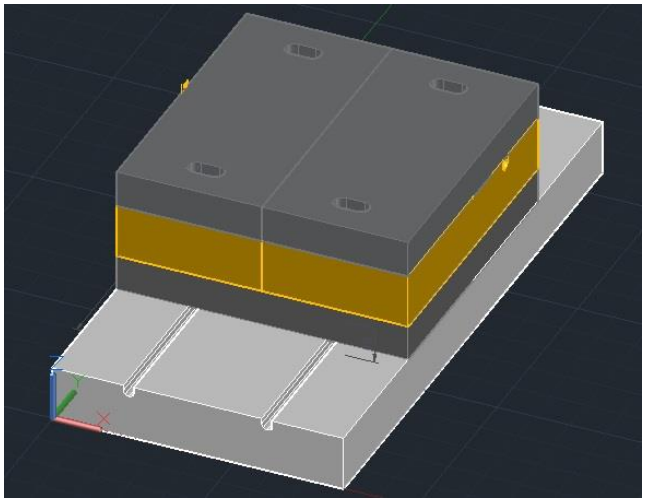

Fig. I.10 – Solid sketch of the cutting machine.

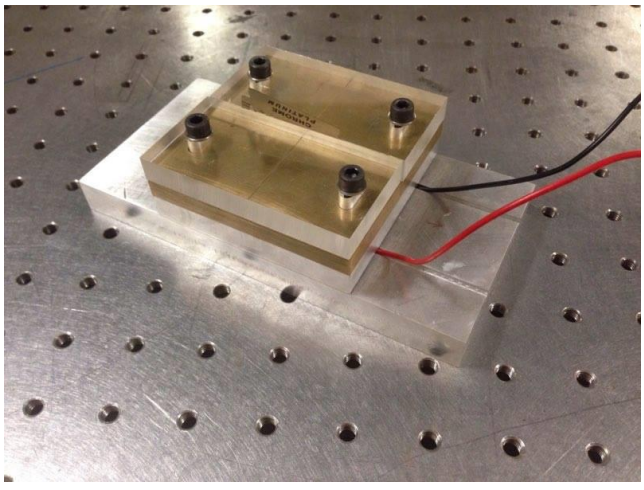

Fig. I.11 - Final result.

Fig. I.12 - An example of a cut.

I.4. T-V Calibration

A calibration was made in voltage (Fig. I.13 a)) and current (Fig. I.13 b)) to assess what voltage or current should be used to heat up the cutting board to the desired 73 ºC.

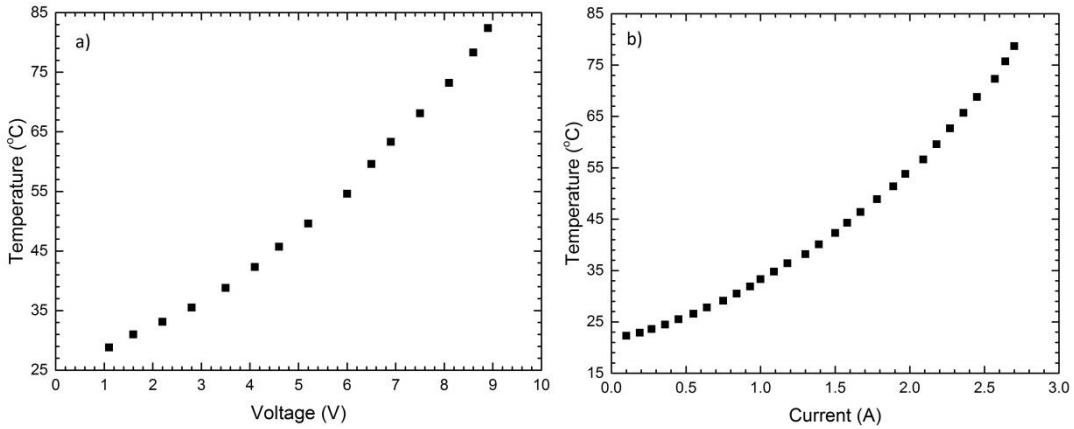

Fig. I.13 - a) Temperature with increasing Voltage. Room temperature equal to 23.6 °C. b) Temperature with increasing Current. Room temperature equal to 21.2 °C.

To keep the temperature around 73 °C is best to regulate the voltage to around 8 V or the current to around 2.5 A. Since the increase of the temperature to the desired temperature isn't an instantaneous effect an analysis was made to check the temperature evolution in time setting the voltage to 7.4 V (Fig. I.14).

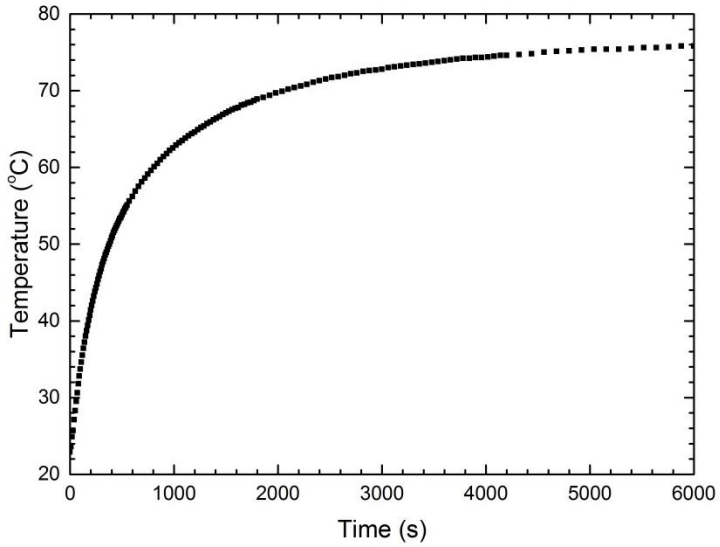

Fig. I.14 - Temperature evolution in time at 7.4 V. Room temperature equal to 22.9 °C.

The temperature increases quickly at first, but it takes a long time to stabilize. The best course of action while heating up is to use higher voltages first and then reduce to the voltage that corresponds to the desired temperature.

References

[1] R. Tricker, *Optoelectronics and fiber optic technology*. Newnes, 2002.

[2] G. D. Peng, “Prospects of polymer optical fibres and gratings in sensing,” *2002 15th Opt. Fiber Sensors Conf. Tech. Dig. OFS 2002*, no. August, pp. 71–74, 2002.

[3] X. F. Chen, C. Zhang, D. J. Webb, G.-D. Peng, and K. Kalli, “Bragg grating in polymer optical fibre for strain, bend and temperature sensing,” *Meas. Sci. Technol.*, vol. 21, no. 9, p. 094005, 2010.

[4] G. Statkiewicz-barabach, D. Kowal, M. K. Szczurowski, P. Mergo, and W. Urbanczyk, “Hydrostatic Pressure and Strain Sensitivity of Long Period Grating Fabricated in Polymer Microstructured Fiber,” *IEEE Photonics Technol. Lett.*, vol. 25, no. 5, pp. 496–499, 2013.

[5] J. Jensen, P. Hoiby, G. Emiliyanov, O. Bang, L. Pedersen, and A. Bjarklev, “Selective detection of antibodies in microstructured polymer optical fibers.,” *Opt. Express*, vol. 13, no. 15, pp. 5883–5889, 2005.

[6] N. Hirayama and Y. Sano, “Fiber Bragg grating temperature sensor for practical use,” *ISA Trans.*, vol. 39, no. 2, pp. 169–73, 2000.

[7] F. Urban, J. Kadlec, R. Vlach, and R. Kuchta, “Design of a pressure sensor based on optical fiber Bragg grating lateral deformation,” *Sensors*, vol. 10, no. 12, pp. 11212–11225, 2010.

[8] V. Bhatia, “Applications of long-period gratings to single and multi-parameter sensing.,” *Opt. Express*, vol. 4, no. 11, pp. 457–466, 1999.

[9] L. Bilro, N. Alberto, J. L. Pinto, and R. Nogueira, “Optical Sensors Based on Plastic Fibers,” *Sensors*, vol. 12, no. 12, pp. 12184–12207, 2012.

[10] P. Polishuk, “Plastic optical fibers branch out,” *IEEE Commun. Mag.*, vol. 44, no. 9, pp. 1–21, 2006.

[11] G. Beadie, M. Brindza, R. A. Flynn, A. Rosenberg, and J. S. Shirk, “Refractive index measurements of poly(methyl-methacrylate) (PMMA) from 0.4–1.6μm,” *Appl. Opt.*, vol. 54, no. 31, pp. F139–F143, 2015.

[12] D. X. Yang, J. Yu, X. Tao, and H. Tam, “Structural and mechanical properties of polymeric optical fiber,” *Mater. Sci. Eng. A*, vol. 364, no. 1–2, pp. 256–259, 2004.

[13] G.-D. Peng and P. L. Chu, “Polymer Optical Fibre Sensing,” *Opt. Inf. Process. Technol.*, vol. 4929, no. 2002, pp. 303–311, 2002.

[14] A. Othonos, “Fiber Bragg gratings,” *Rev. Sci. Instrum.*, vol. 68, no. 12, p. 4309, 1997.

[15] M. M. Werneck, R. C. S. B. Allil, B. a Ribeiro, and F. V. B. De Nazaré, “A Guide

to Fiber Bragg Grating Sensors," in *Current Trends in Shortand Long-period Fiber Gratings*, 2013, pp. 1–24.

[16] B. A. L. Gwandu, X. W. Shu, Y. Liu, W. Zhang, L. Zhang, and I. Bennion, "Simultaneous measurement of strain and curvature using superstructure fibre Bragg gratings," *Sensors Actuators, A Phys.*, vol. 96, no. 2–3, pp. 133–139, 2002.

[17] A. D. Kersey, M. A. Davis, H. J. Patrick, M. LeBlanc, K. P. Koo, C. G. Askins, M. A. Putnam, and E. J. Friebele, "Fiber grating sensors," *J. Light. Technol.*, vol. 15, no. 8, pp. 1442–1462, 1997.

[18] M. J. Gander, W. N. MacPherson, R. McBride, J. D. C. Jones, L. Zhang, I. Bennion, P. M. Blanchard, J. G. Burnett, and A. H. Greenaway, "Bend measurement using Bragg gratings in multicore fibre," *Electron. Lett.*, vol. 36, no. 2, p. 120, 2000.

[19] G. Chen, L. Liu, H. Jia, J. Yu, L. Xu, and W. Wang, "Simultaneous pressure and temperature measurement using Hi-Bi fiber Bragg gratings," *Opt. Commun.*, vol. 228, no. 1–3, pp. 99–105, 2003.

[20] I. P. Johnson, D. J. Webb, and K. Kalli, "Hydrostatic pressure sensing using a polymer optical fibre Bragg gratings," in *Asia Pacific Optical Sensors Conference*, 2012, vol. 8351, pp. 835106–835106–7.

[21] W. Yuan, A. Stefani, M. Bache, T. Jacobsen, B. Rose, N. Herholdt-Rasmussen, F. K. Nielsen, S. Andresen, O. B. Sørensen, K. S. Hansen, and O. Bang, "Improved thermal and strain performance of annealed polymer optical fiber Bragg gratings," *Opt. Commun.*, vol. 284, no. 1, pp. 176–182, 2011.

[22] K. E. Carroll, C. Zhang, D. J. Webb, K. Kalli, A. Argyros, and M. C. Large, "Thermal response of Bragg gratings in PMMA microstructured optical fibers.," *Opt. Express*, vol. 15, no. 14, pp. 8844–8850, 2007.

[23] V. Bhatia, *Properties and Sensing Applications of Long-Period Gratings*. 1996.

[24] S. W. James and R. P. Tatam, "Optical fibre long-period grating sensors: characteristics and application," *Meas. Sci. Technol.*, vol. 14, no. 5, pp. R49–R61, 2003.

[25] V. Bhatia, "Temperature-insensitive and strain-insensitive long-period grating sensors for smart structures," *Opt. Eng.*, vol. 36, no. 7, p. 1872, 1997.

[26] A. Urrutia, J. Goicoechea, A. L. Ricchiuti, D. Barrera, S. Sales, and F. J. Arregui, "Simultaneous measurement of humidity and temperature based on a partially coated optical fiber long period grating," *Sensors Actuators, B Chem.*, vol. 227, pp. 135–141, 2016.

[27] M. Smietana, W. J. Bock, P. Mikulic, and J. Chen, "Highly sensitive pressure

sensor based on cascaded long-period gratings," in *Sensors, 2012 IEEE*, 2012, pp. 1–4.

[28] L. Zehnder, "Ein neuer Interferenzrefraktor," *Zeitschrift für Instrumentenkd.*, vol. 11, pp. 275–285, 1891.

[29] L. Mach, "Ueber einen Interferenzrefraktor," *Zeitschrift für Instrumentenkd.*, vol. 12, pp. 89–93, 1892.

[30] E. M. Dianov, S. A. Vasiliev, A. S. Kurkov, O. I. Medvedkov, and V. N. Protopopov, "In-Fiber Mach-Zehnder Interferometer based on a pair of Long-Period Gratings," in *ECOC*, 1996, pp. 65–68.

[31] T. Allsop, R. Reeves, D. J. Webb, I. Bennion, and R. Neal, "A high sensitivity refractometer based upon a long period grating Mach-Zehnder interferometer," *Rev. Sci. Instrum.*, vol. 73, no. 4, p. 1702, 2002.

[32] M. C. J. Large, J. Moran, and L. Ye, "The role of viscoelastic properties in strain testing using microstructured polymer optical fibres (mPOF)," *Meas. Sci. Technol.*, vol. 20, no. 3, p. 034014, 2009.

[33] R. Lwin, A. Argyros, S. G. Leon-Saval, and M. C. J. Large, "Strain sensing using long period gratings in microstructured polymer optical fibres," in *21st International Conference on Optical Fibre Sensors (OFS21)*, 2011, vol. 7753, pp. 775394–775396.

[34] A. Argyros, "Microstructured Polymer Optical Fibers," *J. Light. Technol.*, vol. 27, no. 11, pp. 1571–1579, 2009.

[35] G. Durana, J. Gómez, G. Aldabaldetreku, J. Zubia, A. Montero, and I. S. De Ocáriz, "Assessment of an LPG mPOF for strain sensing," *IEEE Sens. J.*, vol. 12, no. 8, pp. 2668–2673, 2012.

[36] D. Kowal, G. Statkiewicz-Barabach, and P. A. M. Ergo, "Inscription of long period gratings using an ultraviolet laser beam in the diffusion-doped microstructured polymer optical fiber," *Appl. Opt.*, vol. 54, no. 20, pp. 6327–6333, 2015.

[37] D. Kowal, G. Statkiewicz-Barabach, P. Mergo, and W. Urbanczyk, "Microstructured polymer optical fiber for long period gratings fabrication using an ultraviolet laser beam," *Opt. Lett.*, vol. 39, no. 8, p. 2242, 2014.

[38] M. A. Van Eijkelenborg, W. Padden, and J. A. Besley, "Mechanically induced long-period gratings in microstructured polymer fibre," *Opt. Commun.*, vol. 236, no. 1–3, pp. 75–78, 2004.

[39] J. Witt, M. Breithaupt, J. Erdmann, and K. Krebber, "Humidity sensing based on microstructured POF long period gratings," in *Proceedings of the International Conference on Plastic Optical Fibres (POF 2011)*, 2011, no. 1, pp. 409–414.

[40] T. a Birks, J. C. Knight, and P. S. Russell, "Endlessly single-mode photonic

crystal fiber.," *Opt. Lett.*, vol. 22, no. 13, pp. 961–963, 1997.

[41] M. van Eijkelenborg, M. Large, A. Argyros, J. Zagari, S. Manos, N. Issa, I. Bassett, S. Fleming, R. McPhedran, C. M. de Sterke, and N. a Nicorovici, "Microstructured polymer optical fibre.," *Opt. Express*, vol. 9, no. 7, pp. 319–327, 2001.

[42] A. Argyros, M. a van Eijkelenborg, M. C. J. Large, and I. M. Bassett, "Hollow-core microstructured polymer optical fiber.," *Opt. Lett.*, vol. 31, no. 2, pp. 172–174, 2006.

[43] M. K. Szczurowski, T. Martynkien, G. Statkiewicz-Barabach, W. Urbanczyk, and D. J. Webb, "Measurements of polarimetric sensitivity to hydrostatic pressure, strain and temperature in birefringent dual-core microstructured polymer fiber.," *Opt. Express*, vol. 18, no. 12, pp. 12076–87, 2010.

[44] P. Mergo, T. Martynkien, and W. Urbanczyk, "Polymer optical microstructured fiber with birefringence induced by stress-applying elements," *Opt. Lett.*, vol. 39, no. 10, pp. 3018–3021, 2014.

[45] K. O. Hill and G. Meltz, "Fiber Bragg Grating Technology Fundamentals and Overview," *J. Light. Technol.*, vol. 15, no. 8, pp. 1263–1276, 1997.

[46] K. O. Hill, B. Malo, F. Bilodeau, D. C. Johnson, and J. Albert, "Bragg gratings fabricated in monomode photosensitive optical fiber by UV exposure through a phase mask," *Appl. Phys. Lett.*, vol. 62, no. 10, pp. 1035–1037, 1993.

[47] B. Malo, K. O. Hill, F. Bilodeau, D. C. Johnson, and J. Albert, "Point-by-point fabrication of micro-Bragg gratings in photosensitive fibre using single excimer pulse refractive index modification techniques," *Electron. Lett.*, vol. 29, no. 18, p. 1668, 1993.

[48] A. Stefani, M. Stecher, G. Town, and O. Bang, "Direct writing of fiber Bragg grating in microstructured polymer optical fiber," *IEEE Photonics Technol. Lett.*, vol. 24, no. 13, pp. 1148–1150, 2012.

[49] I.-L. Bundalo, K. Nielsen, C. Markos, and O. Bang, "Bragg grating writing in PMMA microstructured polymer optical fibers in less than 7 minutes.," *Opt. Express*, vol. 22, no. 5, pp. 5270–6, 2014.

[50] Z. Xiong, G. D. Peng, B. Wu, and P. L. Chu, "Highly Tunable Bragg Gratings in Single-Mode Polymer Optical Fibers," *IEEE Photonics Technol. Lett.*, vol. 11, no. 3, pp. 352–354, 1999.

[51] H. Y. Liu, H. B. Liu, G. D. Peng, and P. L. Chu, "Observation of type I and type II gratings behavior in polymer optical fiber," *Opt. Commun.*, vol. 220, no. 4–6, pp. 337–343, 2003.

[52] G. Statkiewicz-Barabach, D. Kowal, P. Mergo, and W. Urbanczyk, "Comparison

of growth dynamics and temporal stability of Bragg gratings written in polymer fibers of different types," *J. Opt.*, vol. 17, no. 8, p. 85606, 2015.

[53] A. Bar-cohen, B. Han, and K. J. Kim, "Thermo-Optic Effects in Polymer Bragg Gratings," in *Micro- and Opto-Electronic Materials and Structures: Physics, Mechanics, Design, Reliability, Packaging*, 2007, pp. 65–110.

[54] G. H. Meeten and A. N. North, "Refractive index measurement of absorbing and turbid fluids by reflection near the critical angle," *Meas. Sci. Technol.*, vol. 214, no. 5, pp. 441–447, 1991.

[55] C. Gouveia, P. A. S. Jorge, and J. M. Baptista, "Fabry – Pérot Cavity Based on a High-Birefringent Fiber Bragg Grating for Refractive Index and Temperature Measurement," *IEEE Sens. J.*, vol. 12, no. 1, pp. 17–21, 2012.

[56] O. Frazão, T. Martynkien, J. M. Baptista, J. L. Santos, W. Urbanczyk, and J. Wojcik, "Optical refractometer based on a birefringent Bragg grating written in an H-shaped fiber," *Opt. Lett.*, vol. 34, no. 1, pp. 76–78, 2009.

[57] O. Frazão, P. Jorge, J. M. Baptista, and J. L. Santos, "Optical refractometer based on a Hi-Bi D -type fiber loop mirror," in *IEEE Sensors*, 2008, pp. 957–960.

[58] S. F. O. Silva, O. Frazão, P. Caldas, J. L. Santos, F. M. Araújo, and L. A. Ferreira, "Optical fiber refractometer based on a Fabry- Pérot interferometer," *Opt. Eng.*, vol. 47, no. May 2008, pp. 1–5, 2008.

[59] M. Châu, P. Huy, G. Laffont, V. Dewynter, P. Ferdinand, P. Roy, J. Auguste, D. Pagnoux, W. Blanc, and B. Dussardier, "Three-hole microstructured optical fiber for efficient fiber Bragg grating refractometer," *Opt. Lett.*, vol. 32, no. 16, pp. 2390–2392, 2007.

[60] S. C. Warren-smith and T. M. Monro, "Exposed core microstructured optical fiber Bragg gratings : refractive index sensing," *Opt. Express*, vol. 22, no. 2, pp. 28625–28630, 2014.

[61] C. R. Zamarreño, P. Sanchez, M. Hernaez, I. Del Villar, C. Fernandez-Valdivielso, I. R. Matias, and F. J. Arregui, "Dual-Peak Resonance-Based Optical Fiber Refractometers," *IEEE Photonics Technol. Lett.*, vol. 22, no. 24, pp. 1778–1780, 2010.

[62] D. Monzón-Hernández and J. Villatoro, "High-resolution refractive index sensing by means of a multiple-peak surface plasmon resonance optical fiber sensor," *Sensors Actuators, B Chem.*, vol. 115, no. 1, pp. 227–231, 2006.

[63] S. Pevec and D. Donlagic, "High resolution, all-fiber, micro-machined sensor for simultaneous measurement of refractive index and temperature," *Opt. Express*, vol. 22, no. 13, pp. 5764–5769, 2014.

[64] G. Statkiewicz-Barabach, K. Tarnowski, D. Kowal, P. Mergo, and W. Urbanczyk,

"Fabrication of multiple Bragg gratings in microstructured polymer fibers using a phase mask with several diffraction orders," *Opt. Express*, vol. 21, no. 7, pp. 3155–3164, 2013.

[65] P. Michel, J. Dugas, J. M. Cariou, and L. Martin, "Thermal variations of refractive index of PMMA , polystyrene , and poly (4-," *J. Macromol. Sci. Part B Phys.*, vol. 25, no. 4, pp. 379–394, 2006.

[66] T. Wei, Y. Han, Y. Li, H. Tsai, and H. Xiao, "Temperature-insensitive miniaturized fiber inline Fabry-Perot interferometer for highly sensitive refractive index measurement," *Opt. Express*, vol. 16, no. 8, pp. 14123–14128, 2008.

[67] C. Wochnowski, S. Metev, and G. Sepold, "UV-laser-assisted modification of the optical properties of polymethylmethacrylate," *Appl. Surf. Sci.*, vol. 154, no. September, pp. 706–711, 2000.